UCRL-317
Copy 2.

UNCLASSIFIED

Radio Frequency Accelerating System for the 300 Mev Synchrotron

By

Craig Spencer Nunan
B.S. (University of California) 1940

THESIS

Submitted in partial satisfaction of the requirements for the degree of

MASTER OF SCIENCE

in

Electrical Engineering

in the

GRADUATE DIVISION

of the

UNIVERSITY OF CALIFORNIA

Approved:

.....

.....

.....

Committee in Charge

Deposited in the University Library.....
Date Librarian

DISCLAIMER

This document was prepared as an account of work sponsored by the United States Government. While this document is believed to contain correct information, neither the United States Government nor any agency thereof, nor the Regents of the University of California, nor any of their employees, makes any warranty, express or implied, or assumes any legal responsibility for the accuracy, completeness, or usefulness of any information, apparatus, product, or process disclosed, or represents that its use would not infringe privately owned rights. Reference herein to any specific commercial product, process, or service by its trade name, trademark, manufacturer, or otherwise, does not necessarily constitute or imply its endorsement, recommendation, or favoring by the United States Government or any agency thereof, or the Regents of the University of California. The views and opinions of authors expressed herein do not necessarily state or reflect those of the United States Government or any agency thereof or the Regents of the University of California.

TABLE OF CONTENTS

List of Illustrations Page 3

Acknowledgments 5

Introduction 7

Chapter I, Synchrotron Theory and Specifications for the Accelerator System 11

Chapter II, The Resonator

A. Design 17
B. Preparation 24
C. Q Measurements 28
D. Eddy Current Measurements 33

Chapter III, The Oscillator 36

Chapter IV, Operation in the Synchrotron 45

Summary 51

Bibliography 52

LIST OF ILLUSTRATIONS

Figure

1. Accelerating system for phenolic vacuum chamber.

2. End view of accelerating grids for phenolic vacuum chamber.

3. The quartz vacuum chamber.

4. Curves of minimum r.f. accelerating voltage.

5. Sketches for eddy current calculations.

6. Graphs of eddy current magnetic fields.

7. Equipment for measuring Q.

8. Test arrangement of pole tip wedges and resonator.

9. Copper model of quartz resonator, top half opened.

10. Copper model of quartz resonator, completed.

11. Smoothed plot of current flow lines in unscribed copper model of quartz resonator.

12. Quartz resonator #1, showing positions of cross-strap for Q measurements.

13. Table of Q measurements.

14. Equipment for measuring eddy current magnetic field.

15. Schematic wiring diagram of exciter used in eddy current tests.

16. Eddy current field of vertically scribed resonator #1.

17. Eddy current field of radially scribed resonator #2.

18. Schematic diagram of pulser for r.f. oscillator.

19. Schematic diagram of r.f. oscillator.

20. Calculated standing voltage wave on transmission line of first test oscillator.

21. Calculated standing voltage wave on transmission line with zircon transformer.

22. Constant current characteristics of 3X2500A3 triode.

23. Calculated 3X2500A3 operating voltages and currents.

Figure

24. R.f. test oscillator with zircon transformer.

25. R.f. test oscillator and resonator #1.

26. Quartz resonator #2, showing radial scribing and feedpoint arrangement.

27. Left side of final oscillator installed in synchrotron.

28. Left side of final oscillator, covers removed.

29. Right side of final oscillator.

30. Right side of final oscillator, cover removed.

31. Top view of final oscillator.

32. Curve of synchrotron beam intensity vs. oscillator frequency.

33. Curve of synchrotron beam intensity vs. r.f. oscillator pulse turn-on time.

34. Curve of synchrotron beam intensity vs. r.f. voltage at quartz resonator gap.

35. Envelopes of r.f. voltage for pulse shaping tests.

36. Photograph of synchrotron x-ray beam.

37. Artist's sketch of cross-section of synchrotron.

38. Drawing of recommended scribing arrangement of quartz resonator.

39. Assembly drawing of final oscillator.

ACKNOWLEDGMENTS

The work described in this report was performed under the auspices of the Atomic Energy Commission. Dr. A. Carl Helmholz was in charge of the project. J. V. Franck and J. M. Peterson developed the complete r.f. system for the phenolic walled vacuum chamber. While this system was being tried in the synchrotron, M. H. Dazey and C. S. Nunan started development of the quartz vacuum system, resonator and oscillator. When the phenolic walled system was discarded in favor of the quartz vacuum chamber, Peterson returned part time and Franck full time to development of the quartz system. In a truly group project such as this there is much overlapping of ideas and each man contributes in part to every phase of the problem. It is therefore impossible to give specific credit. Very generally, individual responsibility can be categorized as follows:

(a)	M. H. Dazey	Construction of early test oscillators. Development of metal firing techniques for quartz vacuum systems. Some Q measurements. Contributions to design of each phase of the system.
(b)	J. V. Franck	Design of first pulser. Aid in power tests of all oscillators. Design of zircon transformer. Contributions to design of test oscillators and resonator. Design of final oscillator installed in synchrotron.
(c)	J. M. Peterson	Design of first pulser. Design of eddy current testing magnet. Eddy current tests. Contributions to design of oscillator transmission line and resonator scribing.

(d) C. S. Nunan — Calculation of eddy current fields.

Design of the quartz resonator scribing.

Q measurements.

Current flow lines in air dielectric model resonator.

Design and power testing of the test oscillators.

Design of the final pulser.

Tests of oscillator performance in the synchrotron.

Design of r.f. voltage pulse shaping equipment.

In addition, W. Basinger aided in scribing the resonators, did all of the copper plating and constructed the air dielectric model resonator.

All of the text and illustrations of this report are the work of the author.

Craig S. Nunan

Berkeley, California
March 26, 1949

INTRODUCTION

The synchrotron principle was proposed by V. Veksler[1] in an article received March 1, 1945, by the Journal of Physics (U.S.S.R.). Veksler pointed out that considerably higher energies could be obtained with the synchrotron than with the betatron because the r.f. accelerator field would supply the extra energy necessary to compensate for the radiation loss of the electrons. In the betatron the maximum energy is limited to the value where the electrons lose as much energy by radiation as they gain per turn from the time rate of change of enclosed magnetic field.

Without prior knowledge of Veksler's article, in letters of September 5 and 9, 1945, to the editor of the Physical Review, E. M. McMillan[2] proposed the synchrotron principle. McMillan suggested a possible design for a 300 Mev electron accelerator which involved injection at 300 kv, r.f. acceleration from injection to 300 Mev, and orbit expansion from 78 to 100 centimeters.

H. C. Pollock[3] suggested injection at 50 to 100 kv, betatron acceleration to 2 Mev and r.f. acceleration the rest of the way to 300 Mev. The orbit would expand only 2%, thereby allowing a considerable saving in the size of the magnet and vacuum chamber. Pollock states in his article that W. Powell and D. Bohm at Berkeley had independently noticed the advantage of using betatron acceleration prior to r.f. acceleration.

To check the validity of the proposals of Veksler, McMillan and Pollock, a 4 Mev betatron in Great Britain was converted to synchrotron operation by F. K. Goward and D. E. Barnes[4]. They were able to increase the energy to 8 Mev. The r.f. accelerator was a quarter wave coaxial resonator bent in a 90° arc and installed on the outside of the vacuum

chamber. The resonator was formed of #26 S.W.G. wires 1/16 inch apart shorted only at the anti-node. The r.f. electric field was inhomogeneous since only wires of resonant length were strongly excited. There was r.f. power loss in the aquadag coating on the inside of the porcelain vacuum chamber and loss in the magnet iron near the resonator. The r.f. electric field caught and accelerated about 25% of the betatron beam. The resonator was excited by a CW oscillator feeding a buffer amplifier at 640 mc. Less than 100 volts was developed at the resonator gap and the buildup time to full voltage was about 10 microseconds.

F. R. Elder, A. M. Gurewitsch, R. V. Langmuir and H. C. Pollock[5] built a 70 Mev synchrotron employing initial betatron acceleration. The r.f. accelerator was a 57° sector of the toroidal shaped glass vacuum chamber. It consisted of Corning 707-DG glass coated with silver paint, electroplated with silver and subdivided into longitudinal strips 5 to 8 mm wide to reduce eddy currents. The resonator was matched to a 50 ohm coaxial line and excited by an 832-A oscillator driving an 829-B grid-modulated power amplifier. 1000 volts r.f. was developed across a 1/8 inch gap in the resonator plating. The frequency of the quartz resonator was tuned by sliding a shorting strap along a section of plating which had been scribed to form a transmission line stub. Movement of the shorting bar changed the stub reactance and therefore the resonator frequency. The synchrotron output was found to be fairly constant over an r.f. turn-on time equal to 10% of the betatron acceleration time. The synchrotron output was independent of r.f. envelope rise time over a range from 2 to 20 microseconds and was constant for r.f. voltages above 3 times the minimum r.f. voltage.

A. M. Gurewitsch[6] has also used a resonator on the outside of the vacuum chamber of the above General Electric Company 70 Mev synchrotron.

1.5 mil copper strips were glued to the outside of the vacuum chamber and to the inside of a concentric support structure and were connected to form a quarter wave air dielectric coaxial resonator. The conducting coating on the inside of the vacuum chamber was interrupted for 3 inches adjacent the resonator gap. The Q of the resonator is largely dependent upon the dielectric loss in the glass wall adjacent the gap.

Shortly after McMillan's proposal was published, construction was started on a 300 Mev synchrotron at the University of California. The early design employed a vacuum chamber consisting of laminated pole tips sealed by rubber gaskets to concentric phenolic rings, which were made of glass cloth impregnated with permafil. See Figs. 1 and 2. The best vacuum obtainable with this system was approximately 10^{-4} mm of mercury, which was considered marginal because of excessive gas scattering in the General Electric Company 70 Mev synchrotron when the pressure was raised to this value.

As insurance in case of unsatisfactory operation with the phenolic wall vacuum chamber, sufficient 45° fused quartz segments were purchased to form a toroidal shaped vacuum chamber. See Fig. 3. One of the segments was modified to form a quarter wave coaxial resonator with accelerating gap. The other segments were coated with Dupont #4817 air drying silver solution to prevent collection of static charges on the vacuum wall with consequent deflection of the electron beam. A radio frequency oscillator was developed to excite the quartz resonator. When difficulties were encountered in obtaining a betatron beam with the phenolic walled vacuum chamber, the magnet was disassembled and, after more thorough compensation of the magnetic field was made, the quartz resonator and r.f. oscillator were installed.

This report describes the development of the quartz resonator and r.f. oscillator. From reading this report, it may appear that designs

were all worked out before any construction or experimenting was done and that these designs were so accurate that everything worked the first time. Actually, design, construction and experimenting proceeded concurrently; preliminary models were tried and modifications made before the designs described herein were evolved. Description of the preliminary models and results is omitted for clarity. Even though more or less standard engineering is involved in much of the work, the methods used in making the final designs are emphasized in this report in order that it may form a useful reference for design of similar equipment for other applications.

CHAPTER I, Synchrotron Theory and Specifications for the Accelerator System

The basic idea of the synchrotron involves phase stability in the motion of a charged particle in an axial magnetic and azimuthal alternating electric field. Suppose a particle is revolving in a constant magnetic field, passing through accelerating gaps across which an alternating electric field is applied. Suppose that the particle passes through the accelerating gaps just as the electric field is changing through zero from accelerating to decelerating. The orbit is stationary because the energy is not changing and H_r must remain constant. To show that the orbit is stable, suppose the particle arrives at the gap too early. It is accelerated, which means its relativistic mass, m increases, its angular velocity, ω decreases, its orbit radius increases and the particle falls behind in phase until finally it arrives late enough to be decelerated. Then the energy is decreased by the alternating electric field, m decreases, ω increases, r decreases and the particle moves ahead in phase, again passing through the equilibrium phase.

$$(1) \quad \omega = \frac{e\,H_{axial}}{m} \text{ e.m.u.} = \frac{e\,c\,H_{axial}}{E} \text{ (e.s.u.)}$$

where E is the total energy, including rest energy. Acceleration can be accomplished by slowly increasing the magnetic field. Veksler[1] states that automatic phasing will exist if

$$\frac{dH}{dt} \ll \frac{4\pi V_0}{T_\lambda^2\, c}$$

where dH/dt is the rate of change of magnetic field at the orbit, V_0 is the peak amplitude of the r.f. gap voltage and T_λ is the period of oscillation of the r.f. field. The electrons will gain just enough energy from the r.f. electric field each turn to stay in step with the magnetic field. The phase stable electron bunch passes through the

$\omega H_{max} = \frac{dH}{dt}(max)$

$3.77 \times 10^4 = 3.77 \times 10^6$ at 60 ~

1.5×10^6 at injection

due to slow down

at injection.

accelerating gap during the second quarter of each cycle when the gap voltage is decreasing from peak value to zero.

In order to have radial and axial stability of the electron orbit, the magnet pole tips are shaped so the magnetic field bows radially outward. The magnet field shape is given by Kerst and Serber[7] as:

$$(2) \qquad H_z = H_o(t)\left(\frac{r_o}{r}\right)^m$$

where $H_o(t)$ is the axial component of magnetic field at the equilibrium radius r_o. H_z is the axial component of magnetic field at the radius r. For radial focusing, n must be less than unity; for axial stability n must be greater than zero.

In the University of California synchrotron, the magnetic field is varied sinusoidally at either a 30 or 60 cycle rate and the frequency of the electric field is held constant. The peak magnetic field is 10,000 gauss, corresponding to an electron energy of 300 Mev at 100 centimeters radius. The rate of change of magnetic field is $.75 \times 10^6$ gauss/sec. for 30 cycle rate or 1.5×10^6 gauss/sec. for 60 cycle rate. When the magnetic field has increased to 11.2 gauss electrons are injected by a diode gun at 100 kv, giving the electrons a velocity 55% the velocity of light. The electrons are accelerated by betatron action to 2 Mev, 98% the velocity of light. The voltage gained per turn by the electrons due to the rate of change of field enclosed by the orbit is about 500 volts at the 30 cycle rate, 1000 volts at the 60 cycle rate. When the flux bars in the center of the machine begin to saturate, the betatron accelerating voltage decreases and the rate of rise of magnetic field in the orbit increases because the inductance of the magnet decreases. The electrons spiral in to smaller radii. When the electrons have spiralled in to the synchronous radius (98 cm at 47.7 mc) the r.f. gap voltage is turned on. During the r.f. accelerating period the electron velocity increases to almost the velocity of light and the radius increases

to 100 cm at 47.7 mc. The r.f. gap voltage is turned off before the magnetic field reaches maximum and the electrons spiral in to strike the target, producing x-rays in a well collimated beam tangential to the orbit.

Neglecting electron radiation loss, the energy gained per turn is derived from (1) as:

$$(3)\Delta E_s = \frac{e\,c\,\dot{H}_z}{2\pi f^2} \text{ ergs} = \frac{300\,c\,\dot{H}_z}{2\pi f^2} \text{ electron volts per turn}$$

McMillan[2] gives the incoherent radiation loss as:

$$(4)\ L = 400\pi\ \frac{e}{r}\left(\frac{E_s}{m_0c^2}\right)^4 \text{ electron volts per turn.}$$

E_s is synchronous energy.

If the betatron accelerating voltage is represented by ΔE_β, the minimum r.f. accelerating voltage is $(\Delta E_s + L - \Delta E_\beta)$. Fig. 4 shows calculated curves of L and $(\Delta E_s + L - \Delta E_\beta)$ and measured curves of ΔE_β for 30 and 60 cycle rates. In order to have phase stability over an azimuthal phase angle ϕ, the r.f. gap voltage should be greater than the curve of Fig. 4 by the ratio $1/\sin\phi$. F. R. Elder, et al[5] found that the General Electric Company 70 Mev synchrotron output increased only 25% for an r.f. gap voltage increase from twice to six times the minimum voltage. F. K. Goward, et al[4] state that to pick up 50% of the betatron beam the r.f. gap voltage should be twice the minimum value. Therefore, the r.f. accelerating system for the University of California synchrotron was designed to produce a nominal gap voltage of 5000 volts, which is a little more than twice the minimum value for 60 cycle rate.

Bohm and Foldy[8] calculate that if the r.f. voltage rises 10 volts per cycle or faster, at least half the particles accelerated during the betatron phase of operation will be trapped in the synchronous orbit. Their calculation assumes:

(a) R.f. turn-on timing jitter of $\pm$ 1 microsecond, corresponding to $\pm$ 850 electron volts spread in betatron beam energy.

(b) Due to the finite time over which injected electrons are accepted into stable orbits, an additional $\pm$ 1.65 Kev spread in betatron beam energy occurs.

Bohm and Foldy[8] show that after the r.f. voltage is turned on, the radial oscillation amplitude is given by:

$$(5) \quad \frac{\Delta r}{r_s} \propto \left[\frac{V}{(1-n)^3 E_s^3} \right]^{1/4}$$

V = r.f. voltage
E_s = synchronous energy
r_s = synchronous radius

This indicates that some gain in synchrotron beam intensity may be expected by shaping the r.f. voltage pulse to rise like the minimum r.f. voltage curve of Fig. 4. However, in order to have phase stability over a large azimuthal angle, a pulse rate of rise of two or three times that shown in Fig. 4 should be used.

Bohm and Foldy[8] show that azimuthal variations, ΔH of magnetic field produce distorted orbits, the maximum deviation x from the instantaneous circle of radius r_i being given by:

$$(6) \qquad \frac{x}{r_i} = \sum_{\ell=1}^{\infty} \frac{\Delta H}{(\ell^2 + n - 1) H} \cos (\ell\theta + \alpha_\ell)$$

where ℓ is the harmonic number of the azimuthal variation and α_ℓ is the phase of the asymmetry. Thus, a single bump (such as might be produced by eddy currents in the r.f. accelerator) in the magnetic field changes a circular orbit to an elongated orbit. Two bumps of equal magnitude, 180° apart produce 18% the distortion that a single bump of the same size produces, for n 2/3.

For an injection voltage of 100 kv, the magnetic field at the betatron orbit is 11.2 gauss. For an orbit deviation of 1 cm, ΔH can be .07 gauss for a first harmonic disturbance or .4 gauss for a second

harmonic disturbance. The eddy current field of the resonator extends over 45° and will be considered uniform over this arc. The amplitude of the nth harmonic of a rectangular recurrent waveform is:

$$C_n = \frac{2\,A\,d}{T}\left[\frac{\sin\frac{n\pi d}{T}}{\frac{n\pi d}{T}}\right] \tag{7}$$

where: A = amplitude of rectangular waveform

d = time over which waveform extends

T = time to recurrence of next waveform

C_n = amplitude of nth harmonic.

For the first harmonic with the resonator uncompensated:

$$C_1 = \frac{A}{4}\left[\frac{\sin\ \pi/8}{\pi/8}\right] = .24A$$

If a field equal to the resonator eddy current field is produced on the diagonally opposite side of the orbit, the first harmonic amplitude of the waveform (second harmonic of the electron orbit) is:

$$C_1 = \frac{A}{2}\left[\frac{\sin\ \pi/4}{\pi/4}\right] = .45A$$

Thus, for 1 cm deviation of the electron orbit, the uncompensated eddy current field of the resonator can be .07/.24 = .3 gauss. If a similar field is produced diagonally opposite the resonator, the resonator field can be .4/.45 = .9 gauss. Therefore, it was planned to compensate the resonator field with coils which would produce a uniform field (except for radial variation due to n) either at the resonator or on the diagonally opposite side of the orbit. Neglecting the second order effect of the variation in eddy current field due to the variation of the exciting field with radius, the resonator eddy current field should be uniform within ± .3 gauss. For ease of compensation the average eddy current field should not exceed .9 gauss.

The vacuum chamber has minimum and maximum inner radii of 93.5

cm and 106.5 cm. A tuning range from 51.1 mc to 44.9 mc was specified to allow setting the synchronous orbit at any radius in the vacuum chamber.

The basic specifications for the oscillator are summarized below:

(a) Nominal frequency = 47.7 mc; variable from 44.9 mc to 51.1 mc.

(b) Resonator gap voltage = 5000 volts maximum, variable from 500 volts.

(c) R.f. voltage pulse length variable from 10 to 8500 microseconds in 25 microsecond steps.

(d) R.f. turn-on time jitter less than ± 1 microsecond.

(e) In a uniform magnetic field rising 1.5 gauss per microsecond, the eddy current magnetic field of the accelerator should be less than .9 gauss average and should be uniform within ± .3 gauss.

CHAPTER II, The Resonator

A. DESIGN

At 47.7 mc, the dielectric constant and loss factor of fused quartz are 4.0 and .0004 respectively. Since the velocity of propagation of the TEM wave in a coaxial resonator is $C/\sqrt{\mu\epsilon}$, the angular velocity of the wave in the quartz will be 1/2 the angular velocity of the synchrotron electrons. Therefore, the quarter wave resonator must be 1/8 of a circle for operation at 47.7 mc. The resonator could be 1/16 or 1/32 of a circle for 2 or 4 bunches of electrons in the orbit, but the fundamental wavelength was chosen because of greater ease in obtaining r.f. power.

Skin depth in copper plating:

(8) $$\delta = \frac{1}{\sqrt{\pi f \mu \sigma}} \text{ cm} \qquad \begin{array}{l} f = 47.7 \text{ mc} \\ \mu = 4\pi \times 10^{-9} \\ \sigma = .581 \times 10^{6} \text{ mho/cm} \end{array}$$

$$\delta = 9.5 \times 10^{-4} \text{ cm} = .375 \text{ mil.}$$

If the copper plating is one skin depth thick, $1/e^2$ or 13% of the power in the wave propagates through the copper plating. This limits the maximum Q of the resonator to 7. A plating thickness of 1.13 mil allows a maximum Q of 400; 1.5 mils, a Q of 3000. Since operating Q's of the order of 500 are desired, it is necessary to keep the plating thickness greater than 1.5 mils. To allow for irregularities in plating, a nominal thickness of 3 mils was chosen.

The dielectric Q of the resonator is:

(9) $$Q_D = 2\pi f \frac{\text{Energy stored}}{\text{Energy lost per second}} = 2\pi f \frac{\frac{1}{2} C V^2}{\frac{1}{2}\frac{V^2}{X} \cdot \text{loss factor}}$$

$$Q_D \quad \frac{1}{\text{loss factor}}$$

Resistance per radian of the resonator is:

(10) $$R = \frac{2}{\pi} \frac{\ell}{\sigma \delta} \left(\frac{1}{C_o} + \frac{1}{C_1} \right)$$

where: ℓ = length of resonator

C_o = outside circumference

C_i = inside circumference

The loss in the copper per second is:

$$(11) \quad W_c \int_0^{\pi/2} \left(\frac{V_{GAP}}{Z_o} \cos \theta\right)^2 \frac{R}{2}\, d\theta = \frac{\pi}{8} \frac{V^2_{GAP}}{Z_o^2} R$$

$$(12) \quad Z_o = \frac{60}{\sqrt{\epsilon}} \ln \frac{C_o}{C_i}$$

Assuming for simplicity that the resonator cross-section is circular, the capacity per radian of the resonator is:

$$(13) \quad C = \frac{2}{\pi} \ell \frac{.555\,\epsilon}{\ln \frac{C_o}{C_i}}$$

The energy stored in the resonator is:

$$(14) \quad W_s = \int_0^{\pi/2} (V_{GAP} \sin \theta)^2 \frac{C}{2}\, d\theta = \frac{\pi}{8} V^2_{GAP}\, C$$

The Q of the copper is:

$$(15) \quad Q_{Cu} = 2\pi f \frac{W_s}{W_e} = 2\pi f \frac{C}{R} Z_o^2$$

The Q of the copper can also be written as:

$$(16) \quad Q_{Cu} = \frac{2\pi f}{R} \cdot 10^{-7} \ln \frac{C_o}{C_i} \approx \frac{2\pi f}{R} \cdot 10^{-7} \left(\frac{2\pi t}{C_i}\right)$$

The last form is accurate to 2% for dielectric thickness t less than 1/30 the inner circumference C_i. This shows the advantage of having the quartz as thick as practicable without reducing the beam aperture excessively.

Another way of writing the equation for copper Q is:

$$(17) \quad Q_{Cu} = 2\pi^{5/2} \cdot 10^{-7} \frac{t\, C_o}{(C_i + C_o)} \left(\frac{\sigma}{\mu}\right)^{1/2} \frac{f^{1/2}}{\ell} \left(t < \frac{C_i}{30}\right)$$

Since ℓ is inversely proportional to frequency for a quarter wave resonator, the Q of the copper plating is proportional to the 3/2

power of frequency if the inner and outer circumferences are kept constant.

The total Q of the resonator is:

(18) $$Q_{TOTAL} \frac{1}{\frac{1}{Q_{Cu}} + \frac{1}{Q_D}}$$

The impedance at the gap is:

(19) $$Z_{GAP} = \frac{4}{\pi} Q Z_o$$

The power into the resonator is:

(20) $$P = \frac{V^2_{GAP}}{2 Z_{GAP}}$$

The quartz segments used for resonators had an average thickness of 1.2 cm, 41.0 cm outside circumference, 33.3 cm inside circumference, and were plated to have a length along the centerline of 75 cm. The dielectric constant and loss factor of the quartz were 4.0 and .0004, respectively. Using the above equations:

$$Q_{Cu} = 1260$$

$$Q_D = 2500$$

$$Q_{TOTAL} = 840$$

$$Z_o = 6.2 \text{ ohms}$$

$$Z_{GAP} = 6600 \text{ ohms}$$

As indicated in section C of this chapter, the final measured Q of the first quartz resonator was 225 with the resonator installed between the magnet pole tips. Using this figure for Q:

$$Z_{GAP} = 1780 \text{ ohms}$$

The r.f. pulse power into the resonator for 5000 volts at the gap is 7.0 kw. The average power assuming a maximum of 6 pulses per second, each pulse 8500 microseconds long is 360 watts.

Calculation of Eddy Current Magnetic Fields:

It was planned to scribe the copper plating lengthwise, leaving a cross-strap to tie the lengthwise strips together. It was thought to be desirable to place the cross-strap near the feed-point for ease of frequency pulling. It was also planned to arrange the scribe lines vertically so that the center-lines of the vertically displaced longitudinal strips do not form a U in the horizontal plane, with the cross-strap tieing the ends of the U together to form an eddy current loop. See Fig. 5(a).

(a) For an elementary loop of a long thin strip (Fig. 5(b)):

$$V = 2\,\dot{B}\,l\,x \cdot 10^{-8} \text{ volt}$$

$$R = \frac{2\,l\,\rho}{t\,dx}$$

$$i = \frac{V}{R} = \frac{\dot{B}\,t}{\rho} \cdot 10^{-8}\,x\,dx$$

(21) $$dH_v = \frac{.2\,i}{r}\,\frac{x}{r} = \frac{.2\,\dot{B}\,t}{\rho} \cdot 10^{-8}\,\frac{x^2\,dx}{x^2 + D^2}$$

V = volts

R = ohms

ρ = 1.72×10^{-6} ohm cm

t = plating thickness

H_v = vertical field in gauss

$\dot{B}$ = rate of change of field in gauss/sec.

(b) Total vertical field on center-line under one long thin strip:

(22)

$$H_v = \frac{.4\,\dot{B}\,t}{\rho} \cdot 10^{-8} \int_0^{d/2} \frac{x^2 dx}{x^2 + D^2} = \frac{.4\,\dot{B}\,t}{\rho} \cdot 10^{-8}\left[\frac{d}{2} - D\tan^{-1}\frac{d}{2\,D}\right]$$

(23) or

$$H_v = \frac{.4\,\dot{B}\,t}{\rho} \cdot 10^{-8}\left[\frac{d^3}{24\,D^2} - \frac{d^5}{160\,D^4} + \frac{d^7}{1736\,D^6} - \ldots\right]$$

For $d/D < 1/4$ the first term of the series gives accuracy to 1%.

(c) The vertical field at a point displaced from the center plane of a long thin strip (Fig. 5(c)):

$$i = \frac{\dot{B}\,t}{\rho} \cdot 10^{-8}\, x\, dx$$

$$dH_v = \frac{.2\, i}{r}\,\frac{P + x}{r} = \frac{.2\,\dot{B}\,t}{\rho} \cdot 10^{-8}\, x\, dx\, \frac{(P + x)}{(P + x)^2 + D^2}$$

$$H_v = \frac{.2\,\dot{B}\,t}{\rho} \cdot 10^{-8} \int_{-d/2}^{+d/2} \frac{x\,(P + x)}{(P + x)^2 + D^2}\, dx$$

(24)

$$H_v = \frac{.2\,\dot{B}\,t}{\rho} \cdot 10^{-8} \left[d - D\left(\tan^{-1}\frac{(P + d/2)}{D} - \tan^{-1}\frac{(P - d/2)}{D}\right) - \frac{P}{2}\,\ln\frac{(P + d/2)^2 + D^2}{(P - d/2)^2 + D^2} \right]$$

For P = 0, this reduces to the same form as in (b) above.

(d) To obtain the eddy current field from the longitudinal strips at the sides of the resonator, these strips are approximated as in Fig. 5(d):

(25) $$I = \frac{W}{d}\,\frac{\dot{B}\,t}{\rho} \cdot 10^{-8} \int_0^{d/2} x\, dx = \frac{W}{d}\,\frac{\dot{B}\,t}{\rho} \cdot 10^{-8}\,\frac{d^2}{8}$$

$$\frac{I}{2} = \frac{W}{d}\,\frac{\dot{B}\,t}{\rho} \cdot 10^{-8} \int_0^{g} x\, dx = \frac{W}{d}\,\frac{\dot{B}\,t}{\rho} \cdot 10^{-8}\,\frac{g^2}{2}$$

(26) $$\therefore \qquad g = \frac{d}{2\sqrt{2}}.$$

I is the total current in the eddy current loop. g is the horizontal projection of the distance from the center-line of the strip to the "center of gravity of the current." For simplicity in calculating magnetic field, all the current is considered concentrated at the center of gravity.

Summing the contributions from each line of current:

(27) $$H_v = \sum \frac{.2\, I}{r}\,\frac{P}{r}$$

(e) The scribing arrangement and dimensions of Fig. 16 were chosen

(after some calculations with the above equations) as a practical compromise which should satisfy the eddy current requirements and still provide a high Q resonator. Fig. 6 shows radial plots of vertical field in the median plane of the orbit for four 1 cm strips aligned above each other and for the wide strips at the sides of the resonator. A radial plot of the total vertical field is also shown. The variation of total vertical field with height above the median plane has been calculated and found to be constant, within the accuracy of measurement of r, over a vertical range of 5 cm. All values were calculated for a plating thickness of 3 mils and a rate of rise of magnetic field of 1.5 gauss per microsecond during the betatron period, corresponding to 60 cycle operation.

(f) For the cross-strap, the first harmonic component of the peak field is (from equation (7), substituting θ for sin θ because of the small angle):

$$C_1 = \frac{2A}{200\pi} d$$

From equation (23), $H_v = \frac{.4 \dot{B} t}{\rho} \cdot 10^{-8} \left[\frac{d^3}{24 D^2}\right] = A.$

$$C_1 = .53 \cdot 10^{-12} \frac{\dot{B} t}{\rho D^2} d^4. \tag{28}$$

For d = 2.5 cm and t = 3 mils, A = 4.3 gauss at the median plane and C_1 = .034 gauss for four vertically aligned straps, corresponding to an orbit distortion of .45 cm. The vertical field above the median plane has been calculated to give the following orbit distortions: .53 cm 1 cm above, .98 cm 2 cm above and 2.5 cm distortion 3 cm above the median plane.

Heat Developed in the Resonator:

(a) Due to Eddy Currents:

The maximum rate of change of magnetic field occurs after the

betatron period when the flux bars have saturated. Assuming the magnetic field variation is sinusoidal, $\dot{B}_{max} = 3.77 \times 10^6$ gauss/second for the 60 cycle rate.

$$I_{max} = \frac{\dot{B}_{max}\, t}{\rho} \cdot 10^{-8} \frac{d^2}{8} = 20.6 \text{ amperes in the 1 cm strips.}$$

$$I_{max} = \frac{M}{d} \frac{\dot{B}_{max}\, t}{\rho} \cdot 10^{-8} \frac{d^2}{8} = 27 \text{ amperes in the inner and 106 amperes}$$

in the outer side strips.

The peak power loss in the 1 cm strips is:

$$W_{LOSS} = \frac{V^2}{2R} = \frac{1}{2} \int_{-d/2}^{d/2} \frac{4\, \dot{B}^2_{max}\, \ell^2\, x^2 \cdot 10^{-16}}{2 \ell \rho} \cdot \frac{t\, dx}{}$$

$$(29) \qquad W_{LOSS} = \frac{2\, \dot{B}^2_{max}\, \ell\, t}{\rho} \left[\frac{d^3}{24}\right] \cdot 10^{-16} \text{ watts}$$

For ℓ = 75 cm, t = 3 mils, W_{LOSS} = 39 watts per strip. There are 44 such strips. Assuming a maximum of 12 pulses per second, the average power loss from all the 1 cm wide strips is 340 watts. The strips at the sides will have a total average power loss of 70 watts. The total average eddy current power loss for the resonator is 410 watts at the 60 cycle rate with 12 pulses per second.

(b) Due to r.f. power of 7 kw into the resonator for 5000 volts at the gap, the average r.f. power in the resonator with 12 4000 microsecond pulses per second is 340 watts.

The maximum total average power developed in the resonator is then 750 watts. The resonator was cooled by a 200 c.f.m. blower which was calculated to produce a 30 foot per second flow of air over the resonator and to allow a maximum quartz temperature of 70° C for 20° C ambient air. The temperature should not be allowed to exceed 100° C or the plating may come loose due to differential expansion of quartz and metal. Also a low temperature is desired to prevent flow of grease at the vacuum seals.

B. QUARTZ RESONATOR PREPARATION

The quartz segments were purchased from the American Silicate Corporation, Hillside, New Jersey. It is understood that the segments are produced as follows:

(a) A carbon rod is heated electrically to high temperature.

(b) The rod is dipped in a box of silica sand and the particles fuse into a tube around the rod.

(c) This is placed in a cast iron mold which has been lined with refractory sand.

(d) The carbon rod is withdrawn and the tube is blown against the mold by compressed air. The result is an opague fused quartz segment with glazed inside surface and very rough sandy outside surface.

Upon receiving the segments various firing and plating techniques were tried. The following is a list of steps which was found to give the most satisfactory and durable resonator (Fig. 38 shows a recommended scribing arrangement):

(a) Seal off the ends of the segment with thick rubber gaskets and copper end plates pressing against the segment. Fill the inside with concentrated hydrofluoric acid and allow to etch the glazed inside surface for about 8 hours.

(b) With silicon carbide wheels, grind the ends smooth to 45°. Grind the outside surface smooth and to uniform thickness of between 3/8 and 7/16 inch. Grind a groove in the outside surface of the feedbump to accept the outer conductor fingers of the transmission line. With a copper tube and wet carborundum dust, grind a 1 1/8 inch hole for the plug which makes contact to the inner conductor of the transmission line.

(c) Clean the segment thoroughly. Fire in an oven at 1300° F. When cool, paint Hanovia Chemical and Mfg. Co. #05 Liquid Bright Platinum

solution over the whole segment inside and outside except for the gap and the feedbump insulation. Allow to dry at room temperature for one hour. Place in an oven having a small blower for circulation and bring the temperature up uniformly to 1300° F over a period of 4 hours; allow oven to cool over a period of 12 hours. When the segment has cooled to room temperature, paint a second coat and fire similarly. When cool, check the surface resistance with ohmmeter probes over each square inch. If any high resistance spots are found, clean them with sandpaper, repaint and fire. From the time the segment is first cleaned and fired until the electroplating is completed, the segment should be handled with gloves so that skin oils do not hinder firing and plating.

(d) Paint scribe lines on, about 1 mm wide, with red glyptal. The lines are continuous from one end of the segment to the other end, with no cross-strap.

(e) In a copper sulphate solution, electroplate copper 3 mils thick uniformly over the exposed platinum surface. A cyanide plating solution dissolves the platinum. It was found desirable to flash plate at about 15 amperes, using a small movable anode to cover the areas which do not plate from the fixed anodes. After the complete surface is covered with a thin coat, the current is reduced to 5 amperes and the plating is built up uniformly, using movable and fixed anodes.

(f) Clean the red glyptal out of the scribe lines with Methyl Ethyl Ketone.

(g) Clean the platinum and copper out of the scribe lines with a 3/4 x 1/32 inch carborundum disk motor driven through a flexible shaft.

(h) Burn out platinum and copper fingers remaining across the scribe lines by connecting a 5 volt, 200 ampere capacity transformer across adjacent strips of plating, controlling the transformer primary voltage

with a variac. Burn out high resistance fingers by connecting the 110 volt variac output through a 25 watt lamp to adjacent strips. Continue the process until the resistance across each scribe line is higher than 100,000 ohms.

(i) Make the cross-strap by painting 1 inch long, 1/8 inch wide strips over each scribe line at the cross-strap point with Dupont #4817 air drying silver solution.

(j) Paint the whole segment inside and out with three coats of red glyptal except for 3/16 inch wide strips at the cross-strap point.

(k) Electroplate 3 mils of copper on the exposed strips at the cross-strap. Then remove the red glyptal with Methyl Ethyl Ketone.

(l) The coaxial transmission line inner conductor fingers grip a 1 1/8 inch diameter quartz plug which has been platinized and copper plated over the whole surface, leaving no exposed quartz. This plug is now soft soldered vacuum tight to the feedbump. Care must be taken to apply the minimum amount of heat so that the plating does not buckle.

The following are a few of the troubles encountered in developing the above procedure:

(a) If the glazed quartz surface is not etched with hydrofluoric acid, the plating buckles and peels off when the segment is heated with r.f. power.

(b) If the segment is not thoroughly cleaned and fired before painting on the platinum, areas of the platinum film may have high resistance.

(c) If the platinum solution is painted on thick enough to flow, it will run into depressions and blister when fired.

(d) If the oven temperature is raised too fast and a blower or good self-ventilation is not used, a poor platinum coat is obtained. This is probably due to carbonaceous matter being trapped in the flux which fuses

the platinum to the quartz.

(e) Silver plating instead of copper plating has also been tried. The steps are the same as above except that the quartz was fired with Hanovia type MM Liquid Bright Gold and the silver plating was done in a silver cyanide solution. It was found that the silver plating peels off due to mechanical abrasion much more easily than the copper plating. The gold sticks to both the silver and the quartz, so it may be that successive layers of gold are separating.

The instructions in reference (9) have been particularly helpful in obtaining a good platinum surface.

C. Q MEASUREMENTS

Fig. 7 shows the equipment used in measuring the Q of the quartz resonator and current flow lines in the model air dielectric resonator. Fig. 8 shows the test arrangement of pole tip wedges and resonator. The pickup loop was placed in the fringing field at the unplated part of the feedbump. The output of the 35 GT test oscillator was loosely coupled through an 8 inch length of 50 ohm line to a probe at the resonator gap. Q's were determined by measuring the frequencies for half power deflection of the galvanometer. Occasional runs of galvanometer reading vs. frequency were made to check symmetry and freedom from spurious modes. Several lengths of coaxial line between the oscillator and the resonator gap were tried to find a length free from resonances neighboring the 50 mc region of interest.

The calculated Q of the unscribed resonator is 840. The resonator was first platinized and copper plated without scribe lines and the Q was measured as 470 at a frequency of 47.7 mc. After the 3 X 2500 A3 test oscillator was built and power measurements made, the plating was stripped with nitric acid to remove the copper and with aqua regia to remove the platinum. The quartz segment was replatinized and copper plated with scribe lines.

With a cross-strap painted with air-drying silver on both inside and outside surfaces at the inside edge of the gap, the measured Q was 134 when the resonator was away from the pole tips, 36 when between the pole tips. This large reduction in Q from the value for the unscribed resonator was not understood. It appeared at the time that it might be due to the scribe lines cutting across proper current flow lines. Therefore, a twice size air dielectric sheet copper replica of the quart resonator was constructed. See Figs. 9 and 10. Current directions were measured by

finding the position of a pickup loop for zero magnetic field when inserted in the dielectric space. Fig. 11 is a smoothed plot of the current flow lines. Since the maximum deviation from a circular path is about 2 degrees, it was decided that the low Q was not due to distortion of the current flow lines by the scribe lines.

It was also considered that the various strips, being of unequal lengths, would tend to oscillate on different frequencies if less than unity coupling existed between the drive strip and each of the other strips. This would tend to lower the Q. The resonant frequency and Q of the quartz resonator was measured with no cross-strap with the drive probe placed on each strip in turn at the gap. The frequency deviation was .3 mc maximum and the Q varied from 36 to 93 with the resonator away from the pole tip wedges.

The cross-strap was tilted back from the gap at an angle to equalize the lengths of each strip from high current end to cross-strap. This increased the Q between the wedges from 36 to 44. When the gap was widened back to the tilted strap in order to make the electrical length of each strip equal, the Q was still 58. Thus, the increase in Q was due to moving the cross-strap away from the gap. The cross-strap was moved further away from the gap and the Q continued to increase up to the midpoint of the resonator. Further movement of the cross-strap caused the Q to decrease and the Q became dependent upon which strip was being excited by the drive probe at the gap. Fig. 12 shows some of the air drying silver cross-strap positions that were tested. The results of the above two paragraphs indicate that the low Q was not due to the differences in lengths of the various strips.

At first it was thought that because of non-uniformities in quartz thickness, a cross-strap at the midpoint of the resonator would

allow current at the high current end to flow in a strip having large quartz thickness, cross at the midpoint and flow the rest of the way to charge up a strip having small quartz thickness and high capacity. Another possible explanation was that the scribe lines, being vertically displaced, were distorting the electric field lines. The electric field lines could remain radial, ending on current lines which flow down an adjacent outside strip to the midpoint of the resonator, cross and flow the rest of the way to the current antinode in the original strip. If the cross-strap were not near the midpoint, the current in the outside adjacent strip would return to the original strip via electric field lines across the scribe lines. These field lines would bulge up into the pole tip wedges and cause additional losses. However, it appears that the losses due to electric and magnetic field lines escaping through the scribe lines into the wedges were equal since the Q was decreased the same amount for wedges at one end as at the other end of the resonator. The resonator was surrounded with a radiation shield and no change in Q was observed. The third possible cause considered was that the extra capacity of the two bumps near the gap would resonate the side strips at widely different frequencies from the rest of the resonator. This effect was checked roughly by removing the plating from the inside of the inner radius bump. The Q increased 4% and the frequency increased 1.5%, indicating that the two bumps near the gap were only a small part of the total effect which was causing low Q's.

In order to determine the importance of uniformity of quartz thickness and distortion of electric field lines, a second quartz resonator was prepared. A somewhat unsuccessful attempt was made to grind the quartz to uniform thickness. The thickness was held constant within $\pm$ 1/32 inch and grinding to closer tolerances appeared to be an enormous

task. The first resonator was uniform over most of its surface to the same tolerance. The lines were scribed radially. The resulting Q's with this resonator and with the vertically scribed resonator are tabulated in Fig. 13. The radial scribed resonator (Q = 445) is 98% better than the vertically scribed resonator (Q = 225) and has 53% of the calculated Q (840) when installed between the pole tips.

Although many questions are left unanswered as to the cause of lower than calculated Q, the final measured Q's are adequate for the synchrotron application. It appears that the major cause of low Q in the first resonator was the vertical scribing which developed part of the electric field across each scribe line instead of containing all the electric field in the quartz between radially aligned strips of plating. It is difficult to measure with any accuracy the effect of the lumped capacity at the high voltage end due to the two bumps in the quartz. The present data indicates their effect to be of the order of 10%. New quartz segments without these bumps have been purchased and their importance will be determined qualitatively when these segments are plated and scribed. The bumps at the gap in the original quartz segments were ordered merely to make the resonator segments symmetrical with the other segments of the vacuum chamber, thereby simplifying the mold requirements. The remaining discrepancy between calculated and measured Q is probably due to variations in quartz thickness, roughness of the outer quartz surface, thin spots in the plating and non-uniformities in scribing which develop electric fields across the scribe lines and allow magnetic field to leak through the scribe lines. Since the first resonator with no scribe lines had a Q of only 470 as compared to a calculated Q of 840, it appears that further increase in Q will come most readily not from improvement of scribing technique but from improvement of the quartz

surface. If higher Q is ever required, the outside surface of the quartz could be glazed and etched to provide a fairly uniform surface which would hold the plating. It should be noted that resonator #2 with scribe lines and away from the pole tips had a higher Q than resonator #1 without scribe lines. This is probably due to the slightly thicker wall of resonator #2 but indicates that the scribe lines of resonator #2 do not reduce the Q appreciably away from the pole tip wedges.

Part of the reduced Q may be due to an incorrect loss factor. The loss factor of .0004 was obtained from various tables and was not checked experimentally. However, the quartz does not get warm near the gap when it is too hot to touch at the high current end, indicating that the dielectric loss is a small fraction of the total.

D. EDDY CURRENT MAGNETIC FIELD MEASUREMENTS

Fig. 14 shows the test equipment used to measure the eddy current magnetic field of the resonator plating. The iron circuit consists of flux bars and pole tip wedges from the synchrotron. The magnet coil consists of 10 turns of #12 wire around the pole tip wedges, pulsed through GL414 thyratrons by a 50 microfarad condenser bank charged to 700 volts. The thyratrons were triggered 3 times per second by a pulser. The resulting magnetic field produced a signal in a reference peaking strip which triggered the oscilloscope. The schematic diagram of the system is shown in Fig. 15. The magnet was designed to produce a rate of change of magnetic field of 1.5 gauss per microsecond in the air gap. The capacitor bank capacity and power supply voltage were made variable to control the rate of change of field. Two 1 by 10 mil, 1 inch long strips of permalloy were wound with 800 turns of #42 enameled copper wire to form the peaking strip for measuring the time when the magnetic field passed through zero. The output of this peaking strip was fed to the synchroscope vertical deflection amplifier. The peaking strip air core inductance after saturation resonated with the lead and synchroscope capacity to produce a damped oscillation. The time at which the peaking strip output signal passed through zero in the first cycle was used as a measure of the difference between the time when the reference peaking strip triggered the oscilloscope and the time when the magnetic field at a particular point passed through zero. An eddy current would produce a biasing magnetic field which would delay the time at which the field passed through zero. These delay times were measured at various points in the air gap, with and without the resonator installed. At 1.5 gauss per microsecond rate of field change, a 1 microsecond delay corresponds to an eddy current field of 1.5 gauss. Since the eddy current field is proportional to the rate of change of magnetic field, the time delay

produced by a given geometry of plating is independent of the rate of change of field. Therefore, the actual rate of change of magnetic field during the tests is not critical.

The magnet was designed as follows:

A = area of coil around pole tip wedges = 2800 sq. cm.

$\dot{B} = 1.5 \times 10^6$ gauss/sec.

Assuming 20% leakage field, the required voltage per turn is:

$V_{TURN} = A\,\dot{B} \times 1.2 \times 10^{-8} = 50$ volts.

Assuming a 1000 cycle per second resonant frequency, the peak magnetic field is:

$$B_{max} = \frac{\dot{B}}{2\pi f} = 240 \text{ gauss.}$$

Ampere turns $= 2.02 \times B_{max} \times$ Gap height in inches = 1700

With 10 turns, I = 170 amperes and V = 500 volts

$\dot{I} = 1.07 \times 10^6$ amperes per second.

The inductance of the coil around the pole tip wedges is:

$$L = \frac{V}{\dot{I}} = 470 \text{ microhenries.}$$

For resonance at 1000 cycles, the required exciter capacity is:

$$C = \frac{1}{4\pi^2 f^2 L} = 54 \text{ microfarads.}$$

Sufficient flux bars were used to avoid saturation. The force of the magnetic field is:

$$F = \frac{H^2}{8\pi} \text{ dynes/cm}^2 = 14.8 \text{ pounds total.}$$

First and second half cycles of the magnetic field were tried with no measurable difference in eddy current field. Fig. 16 shows the radial and longitudinal variation of eddy current field at the median plane of the vertically scribed quartz resonator #1. Fig. 17 presents the same information for the radially scribed resonator #2 before the scribe

lines numbered 1 and 12 were added. At the time of this writing, due to the flux bars being used continuously in the synchrotron, the eddy current field of #2 resonator with the additional scribe lines has not been measured.

The measured eddy current field from resonator #1 checks fairly well with the calculated field at the center-line of the resonator. See Fig. 6. However, the measured radial variation is much less than the calculated values; this can probably be attributed to a poor approximation of the side strips (Fig. 5(d)). The calculated curves of Fig. 6 indicate that a smaller radial variation would exist if the side strip widths were decreased by adding another scribe line at each side of the resonator. The calculated curves indicate a 30% increase in useful radial aperture would be obtained by adding these extra scribe lines, assuming a maximum allowable variation of magnetic field of ± .3 gauss.

The field of #2 resonator is 60% higher than the field of #1 resonator. Since the fields at the two ends of the resonator are about equal, the loop completed by the cross-strap (Fig. 5(a)) is apparently not contributing very much to the eddy current field. The higher field of resonator #2 can probably be attributed to thicker electroplating.

Assuming a maximum allowable radial variation in eddy current field of ± .3 gauss, the usable radial aperture of resonator #1 is 2.7 inches and the usable aperture of resonator #2 is 3.3 inches.

The field under the cross-strap of resonator #2 is small because the measurements were made when the cross-strap was formed with air drying silver instead of electroplated copper.

No variation of field with height was detected with either resonator but this is not conclusive because of the length of the peaking strip (1 inch).

CHAPTER III, The Oscillator

An oscillator and modulator had already been developed for the accelerator shown in Figs. 1 and 2. Reference (10) is an early progress report of this system. The oscillator used an Eimac 3 X 2500 A3 forced air cooled triode in a grid return circuit and was grid modulated by a pulser of the type shown in Fig. 18. Because the quartz resonator represented a different load problem, extensive modifications of the pulser were required and the oscillator was largely redesigned, keeping the same tube and same general physical arrangement.

The system was first redesigned to energize the unscribed quartz resonator, which had a Q of 470, gap impedance of 3700 ohms and resonant frequency of 47.7 mc. Chapter I gives the basic specifications for the system. In particular, a tuning range from 44.9 to 51.1 mc and resonator gap voltage variable from 500 to 5000 volts were desired. To pull the resonant frequency of the unscribed quartz resonator down to 44.9 mc would require 53 mmfd. at the resonator gap or 4 times this capacity at the feedpoint where the voltage is half the gap voltage. The same reactive energy must be stored in either case for the same shift in frequency, so 4 times the capacity is required at half the voltage. Since eddy current restrictions prohibited placing the tuning condenser at the quartz resonator, the condenser was placed at the oscillator end of the transmission line. By tuning the condenser the voltage node could be moved along the transmission line toward the quartz to add inductive reactance or away from the quartz to add capacitive reactance at the feedpoint. A low impedance transmission line was chosen to keep the movement of the voltage node small so that the transmission line current at the grid loop and voltage at the tube plate would not vary excessively with tuning. A 4½ inch outside diameter, 3½ inch inside diameter, 15.2 ohm transmission

line was chosen for ease of mechanical assembly and freedom from voltage breakdown across insulating spacers. After considerable calculation, a line length of 105 inches was chosen as giving a usable tuning range. A shorter line would put the tube at too low an impedance point for oscillation; a longer line would put the current maximum too far from the grid loop. (The grid loop in the existing oscillator was 26 inches from the tube plate. By completely rebuilding the oscillator, the grid loop could have been placed nearer the current maximum, with consequently larger frequency tuning range.) Fig. 20 shows the calculated voltage standing wave along the transmission line, current at the grid loop and voltage at the tube for various frequencies and 5000 volts across the gap of the unscribed quartz resonator.

The determination of required susceptance to pull the quartz resonator frequency was done by calculating the susceptance at the gap and then multiplying by 4 to get the value at the feedpoint:

$$(30) \quad B = +j \frac{4}{Z_o} \cot\left(\frac{\pi}{2} \frac{f}{f_o}\right)$$

Putting B in per unit of transmission line characteristic admittance and using a Smith chart, the other values listed in Fig. 20 were obtained.

Power tests with this oscillator and the unscribed quartz resonator gave the following results:

Tuning range - 46.5 to 48.5 mc.

Voltage at resonator gap - 6000 volts maximum in vacuum of 10^{-5} mm Hg (gap 3/4 inch wide); 3900 volts in air.

Tube plate voltage - 1800 volts with 3900 volts at gap.

Efficiency - 35% at 47.7 mc with 3900 volts at gap.

This system would not oscillate at plate voltages below 1000 volts, corresponding to 1600 volts at the resonator gap. The system also

oscillated on two spurious modes: 163 mc and 69 mc. The 163 mc mode appeared to be a resonance in the filament leads of the tube and was independent of all tuning. The 69 mc mode occurred only at certain settings of the cathode stem tuning condenser. Both modes were eliminated by installing a 300 ohm, 16 watt globar resistor at the voltage node in the transmission line. Higher resistance allowed the 163 mc mode to exist. Lower resistance loaded the oscillator excessively at frequencies above and below 47.7 mc due to movement of the voltage node.

After the quartz resonator was replated and scribed, the Q was 225, with a gap impedance of 1780 ohms and resonant frequency of 49.7 mc. The gap width was decreased from 3/4 to 3/8 inch to reduce the area which could be charged up by injected electrons which are not focused into the Betatron beam. Unequal charging of the quartz surface would deflect the Betatron beam. With the resonator Q reduced due to scribing, the oscillator would not oscillate because of the low impedance presented to the tube. Therefore, a low impedance coaxial section, using zircon as the dielectric, was inserted in the transmission line to transform the relatively low impedance at the quartz resonator feedpoint to a higher impedance at the tube.

A coaxial quarter-wave section of zircon was copper plated and the resonant frequency and Q were measured to determine the dielectric constant and loss factor. They were 6.3 and .002 respectively at 100 mc and were assumed to be the same at 50 mc. A cylindrical section of zircon 5¼ inches outside diameter, 4½ inches inside diameter was readily available. After some trial calculations, a length of 10.5 inches was chosen. Fig. 21 shows the resulting calculated voltage wave on the transmission line at various frequencies, assuming a minimum total capacity at the tube of 100 mmfd. at 49.7 mc. This capacity requires a 52.5 inch length

of 15.2 ohm transmission line from the zircon transformer to the tube plate for resonance. Note from Fig. 21 that 5800 volts r.f. are now required at the tube for 5000 volts at the resonator gap at 47.7 mc, whereas the earlier design with no zircon transformer required 1500 volts at the tube.

The I^2R loss in the transmission line is approximately equal to the power supplied to the quartz resonator. For 5000 volts at the resonator gap, the total power which the tube must deliver is 14 kw during the pulse. The impedance presented to the tube at 47.7 mc is 1200 ohms. With the earlier oscillator exciting the unscribed resonator with no zircon transformer, the impedance presented to the tube was 235 ohms. Because of the increased impedance at the tube with the zircon transformer, the oscillator should have a higher efficiency and should start oscillating at a lower gap voltage.

Fig. 22 shows the constant current characteristics of the 3 X 2500 A3 triode. Fig. 23 shows the calculated tube voltages and currents assuming 14 kw output at 5800 volts r.f. with a plate current flow angle of 140°.

First harmonic current, $I_1 = \frac{2\ P_{r.f.}}{E_{r.f.}} = 4.8$ amperes.

From page 447 of reference (11), $I_{max} = I_1/.39 = 12.3$ amperes. This establishes one limit of operation on the chart of Fig. 22 at the line of equal plate and grid voltages. In this case it is +400 volts and 4.5 peak amperes grid current. The grid bias for cut-off is about -300 volts at 5500 volts plate voltage. The peak grid-cathode voltage is determined by allowing it to remain above cut-off for 140 degrees:

$E_{G-K} \sin 20^\circ = 300$ volts

$E_{G-K} = 850$ volts

The operating grid-cathode bias is 400-850 = -450 volts or 150% of cut-off bias. Grid current flows for the angle:

$$\theta_g = 180 - 2 \sin^{-1} \frac{E_{BIAS}}{E_{G-K}} = 116^\circ$$

From page 447 of reference (11):

d.c. GRID CURRENT, $I_{g_{d.c.}} = .19\ I_{g_{PEAK}} = .85$ amperes

d.c. PLATE CURRENT, $I_{p_{d.c.}} = .22\ I_{max} = 2.7$ amperes.

The required grid bias resistance is 450/.85 = 530 ohms

The total cathode emission current is .85 + 2.7 = 3.6 amperes

The required d.c. plate voltage is $E_{r.f.} - E_{BIAS} = 5350$ volts

The power input is 3.6 x 5350 = 19.3 kw

Tube efficiency = 14/19.3 = 72%.

The peak grid-cathode voltage required is 850 volts with 440 amperes in the transmission line at 47.7 mc. The feedback loop size was calculated as follows:

$$H = \frac{.2\ I \sin \omega t}{r} \qquad \dot{H} = \frac{.2\ \omega\ I \cos \omega t}{r}$$

$$V = \ell \int_{r_1}^{r_2} \dot{H}\ dr \times 10^{-8} = .2\ \omega \ell\ I \cos \omega t \int_{r_1}^{r_2} \frac{dr}{r} \times 10^{-8}$$

$$V = .4\ \pi\ f\ \ell\ I\ \ln \frac{r_2}{r_1} \cos \omega t \times 10^{-8}$$

Let $r_2 = 2.25$ inches, $r_1 = 1.75$ inches, the outer and inner radii of the transmission line.

$V = 66\ \ell$, where ℓ is the length of the feedback loop in cm.

For V = 850 volts, $\ell = 13$ cm or 5 inches.

The feedback loop was actually made 7 inches long and was made adjustable. The inner conductor of the transmission line was slotted so the loop could be expanded into the inner conductor to couple all of the flux. The loop was formed of ½ inch strap in order to provide a low self-inductance. A condenser was inserted in the feedback loop to allow

tuning to series resonance. The transmission line current lags the tube plate voltage by 90° (neglecting in-phase loss current). The voltage induced in the feedback loop leads the transmission line current by 90°, so is in phase with the tube voltage. With the inductance of the feedback loop resonated by the series condenser, the voltage fed back to the cathode is in phase with the plate voltage. See Fig. 23.

The tuned coaxial quarter-wave stub was added at the cathode for two reasons:

(1) To act as an r.f. choke to allow filament voltage to be fed in at ground potential.

(2) To act as a reservoir of energy to improve the wave shape of the cathode-grid r.f. voltage. The impedance of the feedback loop is high enough to cause a large voltage drop between cathode and grid when current flows. The cathode stub was designed with low characteristic impedance (22 ohms) so that it supplies most of the grid current during the 116° flow angle with small distortion of the cathode-grid voltage from a sinusoid.

The coupling capacitor from the tube plate to the inner conductor of the transmission line consisted of three 1/8 x 6 inch titanium dioxide disks which had been platinized and copper plated. The disks were stacked, with soft copper waffles between each pair for contact to the copper plating. The capacity was measured as 2000 mfd. The voltage drop is approximately 100 volts at full power.

The plate voltage was supplied through a quarter-wave coaxial stub fore-shortened by making the inner conductor a choke. The plate voltage was bypassed at the r.f. voltage node by a 300 mmfd. polystyrene condenser.

The pulser (Fig. 18) was designed to provide pulse lengths

variable from 0 to 8500 microseconds in 25 microsecond steps, except for the first 25 microseconds in which the pulse length is continously variable. The pulse length is quantized by the ringing circuit which uses two 6SN7's and a 6AC7 to put sharp pulses every 25 microseconds on the normal RC voltage decay curve of the first 6AG7 of the multivibrator. The multivibrator circuit is standard. Relay 1 provides quick switching from long to short pulses to facilitate tuning to catch the Betatron beam. V4 is normally conducting. A negative trigger turns off V4, which fires V5 to start the pulse. When V5 conducts,the grid voltage of V8 is driven negative and decays to zero as C_1 discharges; when the ringing circuit pip superimposed on this decay curve can drive the grid of V4 above cutoff, V4 conducts, V5 stops conducting and the plate voltage of V5 rises to supply voltage, ending the pulse. C_2 and R_2 isolate V5 plate from V4 grid voltage so that this rise time is fast.

The 807's are normally conducting to provide fixed bias across R50 for the 3 X 2500 A3 oscillator triode. The start of the multivibrator pulse drives the grids of the 807's below cutoff. The 3 X 2500 A3 grid voltage rises toward ground potential, the time constant of this rise being determined mainly by R3 and the grid to ground capacity of the oscillator. The grids of the 807's are held below cutoff as long as the pulse length by the time constant of C_3 and the grid-to-ground resistors. At the end of the multivibrator pulse when V5 plate potential rises, the grids of the 807's are driven positive and the plate potential of the 807's drops toward the cathode potential. This voltage pulse is transmitted through C_4 to drive the oscillator grid far enough negative so that the r.f. peaks of grid-cathode drive voltage are below cutoff. The time constant of C_4 and R5 is made longer than the time for decay of oscillations so that the r.f. peaks of grid-cathode drive voltage are kept

below cutoff. During the off period between pulses, the oscillator grid voltage is held below cutoff by the current of the 807's flowing through R3. Since a fixed bias a little greater than 300 volts across a 530 ohm resistor is desired according to the oscillator calculations, the 807's should pass a little more than 570 milliamperes; 600 milliamperes is assumed for safety. At the end of the pulse, the oscillator grid voltage must be dropped more than 700 volts and 900 is assumed for safety, making R5 1500 ohms. With C_4 equal to .004 mfd., the time constant is 6 microseconds, which is longer than the decay time of the r.f. envelope. Incidentally, this 6 microsecond time constant limits the minimum length of short pulse to about 10 microseconds at full power because the voltage across C_4 must decay during the pulse in order to transmit the 700 volts minimum to drive the r.f. grid voltage peaks below cutoff. A power supply voltage of 1300 volts is required to supply the fixed bias across R3, pulse stopping voltage across R4 and voltage drop across the 807's.

The tickler oscillator was installed to eliminate jitter in the r.f. envelope starting time. A 2C26A was employed in a Colpitts circuit operating at 100 volts plate voltage. The output was coupled through a probe to the cathode stem of the main oscillator.

Figs. 24 and 25 show the test oscillator constructed according to the above design. Figs. 27 to 31, inclusive, show the final operating model installed in the synchrotron. The results of power tests conducted on each oscillator are essentially similar.

The oscillator has a tuning range from 46.4 to 49.1 mc with only the transmission line condenser being tuned, the cathode and feedback loop condensers being set for the middle of the range. If the cathode and feedback loop condensers are retuned every 2 or 3 mc, the oscillator operates properly over the full range of the transmission line tuning

condenser, 44.6 to 50.4 mc.

The maximum voltage obtained in vacuum of better than 10^{-5} mm of mercury is 4000 volts across the 3/8 inch wide gap of the resonator. The maximum gap voltage before sparking at 1 atmosphere pressure is 2300 volts.

To determine oscillator efficiency the temperature rise of the cooling air for various d.c. input powers was measured with the tube oscillating and again with all resonant circuits shorted to stop all modes of oscillation. The efficiency of the tube was found to be about 60% at 2000 volts gap voltage and 47.7 mc.

The r.f. envelope buildup time is approximately 6 microseconds. The jitter is about .2 microsecond without the tickler oscillator and less than .1 microsecond with the tickler oscillator operating.

CHAPTER IV, Operation in the Synchrotron

After a betatron beam was obtained, little difficulty was encountered in catching and accelerating it with the r.f. pulse. The dependence of x-ray beam intensity on r.f. pulse frequency, starting time and voltage is shown in Figs. 32, 33 and 34, respectively.

The betatron beam was monitored with an anthracine crystal covered with aluminum foil and mounted on the end of a lucite rod which projected through a Wilson seal into the inner radius of the quartz vacuum chamber. Electrons striking the anthracine produced light which traveled through the lucite rod to a photomultiplier; the output signal was amplified and presented on a synchroscope screen. With r.f. pulses less than 60 microseconds long the synchrotron beam could be monitored by the anthracine without appreciable reduction in photomultiplier sensitivity due to magnet leakage field. Using long r.f. pulses the synchrotron beam spiralled in to strike a uranium target next to the anthracine crystal, producing x-rays which were monitored by a Zeus ionization chamber.

With the fast rising pulse shape (Fig. 35(a)) and a short r.f. pulse, about 60% of the betatron beam was caught, producing a synchrotron beam which was monitored by the anthracine. That is, 40% of the original signal remained at the betatron beam position on the synchroscope screen and 60% of the original signal was moved out about 60 microseconds to form a second signal.

Reference (5) indicates that the rate of rise of the r.f. envelope was varied from 2 to 20 microseconds without effect on the beam intensity of the General Electric Company 70 Mev synchrotron. W. Abson and L. S. Holmes[12] state that the output of the 14 Mev British synchrotron did not change for a range of 5 to 15 microseconds in the r.f. envelope rise time to half value and that 60% of the betatron beam was

being captured and accelerated. Equation (5) above (which is due to Bohm and Foldy[8]) indicates that radial oscillations at betatron capture will be minimized and good azimuthal phase stability will be obtained if the r.f. envelope is shaped to rise about two or three times the minimum rate shown in Fig. 4. With the normal fast-rising r.f. pulse shape it was found that the least amount of betatron beam was left behind when the r.f. gap voltage was only 400 volts. Of course, the electrons accelerated by the r.f. voltage spiralled into the target in a few microseconds when the minimum voltage curve of Fig. 4 crossed the 400 volt line. Therefore, it seemed desirable to have an r.f. voltage envelope which rose rapidly to 400 volts and then slowly over about 500 microseconds to full voltage of about 2400 volts (twice minimum for 30 cycle per second magnet frequency).

A .35 Henry choke was installed in the plate lead of the oscillator to lengthen the rise time. Luckily, the resulting pulse shape had a fast rise to about 30% of full voltage (See Fig. 35(b)). During the off period between pulses the plate to ground capacity of the oscillator charges to power supply voltage. When the grid of the 3 X 2500 A3 oscillator tube is driven above cutoff bias by the pulser, the plate to ground capacity discharges through the tube to produce the fast rise to 30% voltage. The choke then produces an exponential rise to full voltage, the time constant of this rise being about 200 microseconds. This time constant is determined by the plate resistance of the 3 X 2500 A3 tube and is therefore dependent upon plate voltage and grid drive. With the choke in the plate lead about 80% of the betatron beam was caught and accelerated at optimum r.f. voltage. Fig. 34(b) shows that the r.f. pulse shape with the choke increases the synchrotron beam intensity about 20%. Above 3300 gap volts, the synchrotron beam intensity begins to decrease and the percentage of betatron beam that is caught begins to decrease.

This is probably due to the initial rise being too far above 400 volts.

The pulse shape of Fig. 34(c) was obtained by opening the circuit between power supply and oscillator during the period between pulses with a hydrogen thyratron. This prevented the oscillator plate to ground capacity from charging up and eliminated the fast rise to 30% voltage at the beginning of the pulse. With this smoothly rising pulse shape only 60% of the betatron beam was caught with optimum r.f. voltage and the maximum synchrotron beam intensity was the same as with the fast rising pulse shape of Fig. 34(a).

An anthracine crystal was taped to the envelope of a photomultiplier which was placed in the x-ray beam external to the synchrotron. A one centimeter thick sheet of lead was wrapped around the photomultiplier case so that pair-production electrons produced by x-rays in the lead would strike the anthracine. The output of the photomultiplier was amplified and displayed on a long sweep trace of a synchroscope which was delayed to show only photomultiplier signals produced during the last third of the r.f. pulse. With an r.f. gap voltage of 1400 volts the synchroscope trace was filled with photomultiplier signals. When the r.f. gap voltage was increased to 2000 volts, the number of photomultiplier signals decreased to about 10 per pulse, indicating that most of the electrons captured from the betatron period are accelerated to full synchrotron energy. No photomultiplier signals were observed during the early part of the r.f. pulse.

The emission current from the injector was varied without any effect on the time required for the electrons to spiral in and strike the target after the end of the r.f. pulse. This indicates that the energy loss due to radiation by the electrons is independent of the beam current. J. P. Blewett[13] has found with the General Electric Company 100 Mev

betatron that changing the beam current does not change the rate at which the beam loses energy due to radiation. Blewett states that if the total radiation of a group of N closely spaced electrons is calculated, the net energy radiated is proportional to N^2 since the electric fields add up and the energy is proportional to the square of the net field. The radiation fields due to a continuous stream of electrons is self-canceling so that the net energy radiated is zero. Blewett attributes the existence of radiation in the betatron to statistical fluctuations in the beam density. In an earlier article, L. Arzimovich and I. Pomeranchuk[14] predict incoherent radiation in the betatron due to the spread in electron energies in the beam which causes them to change their relative spacings in one turn by more than the effective wavelength of the radiation. In the synchrotron the electrons are bunched by the r.f. field. Apparently the charge density of the bunch is so small or the energy spread and position fluctuations large enough so that the electrons radiate incoherently. W. K. H. Panofsky has calculated back from measurements of the x-ray beam of the University of California synchrotron and found that the number of electrons per pulse is 3×10^6 for a Zeus reading of 1 roentgen per hour when the Zeus meter is shielded by 1/8 inch of lead. The above measurements of radiation loss versus beam intensity were made with a maximum Zeus meter reading of .3 roentgen per hour. McMillan assumed incoherent radiation loss in his original letter[2] and the curves of Fig. 4 and specifications for the oscillator were made accordingly.

The r.f. pulse length is usually set to accelerate over 90 degrees of the magnetic field sine wave, the electrons spiralling into the target in about 150 microseconds after the r.f. pulse due to energy loss by radiation. The time of intense beam lasts for about 10 microseconds on the external photomultiplier. The electrons would still

spiral inward to strike the target when the r.f. pulse was lengthened to 115 degrees of magnet field sine wave. With longer pulses the electrons spiralled out to strike the injector. The 115 degree transition time corresponds to the 65 degree point on the curve of Fig. 4, where the radiation loss per turn equals the decrease in energy required due to the decreasing magnetic field. The longest r.f. pulse used was 150 degrees of magnetic field sine wave and a strong signal was still obtained with the external photomultiplier even though it was no longer in the tangential x-ray beam produced by electrons striking the injector.

The betatron beam was probed at three places around the vacuum chamber and was found to be contained in an aperture 1 inch high (axial) and 3 inches wide (radial). The 3 inch figure checks fairly well with the expected radial aperture indicated by the eddy current field of quartz resonator #1 as plotted in Fig. 16. (The aperture probing was done with resonator #1 installed in the synchrotron). Kerst and Serber[7] give the frequencies of radial and axial oscillations as:

$$\omega_r = \sqrt{1-n}\ \omega \quad ; \quad \omega_A = \sqrt{n}\ \omega$$

Since there is some coupling between radial and axial oscillations the oscillation amplitudes should be inversely proportional to their frequencies, since the energy in the oscillation remains constant. Thus:

$$\Delta A = \frac{\omega_r}{\omega_A}\ \Delta r$$

Here, $\omega_r = 2\pi$: radial oscillation frequency

$\omega_A = 2\pi$: axial oscillation frequency

ω = angular velocity of electrons

ΔA = amplitude of axial oscillations

Δr = amplitude of radial oscillations

For $n = \frac{2}{3}$, $\Delta A = \frac{1}{\sqrt{2}}\ \Delta r$. For $\Delta r = 3$ inches, $\Delta A = 201$ inches.

An n of 9/10 would be required to explain the 1 inch by 3 inch aperture by

the above considerations. From the calculations and measurements of variation of eddy current field with height, the quartz resonator is expected to provide a 2 inch vertical aperture. The limitation on vertical aperture is not understood but may be due to remnants and eddy currents in the pole tips which are not uniformly compensated over the vertical range by the compensating coils, or it may be due to an n of 9/10 since the n of the magnet is adjustable by changing the current in coils over the pole faces and cannot be measured after these adjustments with the quartz ring in place.

When the oscillator was first installed a 2 microsecond jitter was observed in the starting time of the r.f. pulse when the magnet was energized at nominal voltage. As the magnet current decreased, the amount of jitter decreased. When the magnet was pulsed it shook the oscillator. It was concluded that this shaking caused the grid and filament wires of the oscillator tube to vibrate, with consequent fluctuation of the amplification factor and cut-off bias. Since oscillations begin when the pulser bias voltage decays to oscillator cut-off voltage, fluctuation of the value of cut-off bias would cause jitter. The oscillator was vibration mounted with three 40 pound Lord mounts and vibration and jitter disappeared.

The temperature rise of the quartz resonator with blower running has not exceeded 20° C with 30 cycle magnet operation and 3 kv at the resonator gap. With 60 cycle operation and 5 kv at the gap, a temperature rise of about 50° C would be expected. With the blower turned off the resonator runs hot enough due to eddy currents alone to melt the lubriseal at the rubber boot vacuum joints at each end of the resonator, thereby causing a leak.

SUMMARY

The University of California 300 Mev synchrotron employs a toroidal quartz vacuum chamber. A 45° section of the quartz donut has been metallically coated and scribed to form a quarter-wave coaxial resonator for operation at a nominal frequency of 47.7 mc. An arrangement of scribe lines has been developed to give a Q of 445, with eddy current fields uniform enough to provide a 3 inch usable radial aperture. An oscillator has been developed to provide 5 kv peak r.f. volts across the quartz resonator gap over a frequency range sufficient to tune the synchronous electron orbit to either limit of the radial aperture. R.f. voltage pulse shaping has been tried, with a resultant 20% increase in x-ray beam intensity. About 80% of the betatron beam is caught and accelerated by the r.f. pulse.

None of the r.f. pulse parameters have been found to be particularly critical. When twice minimum r.f. gap voltage is used, an inconsequential fraction of the total x-ray beam is produced during the r.f. pulse, indicating that most of the electrons captured from the betatron beam are accelerated to full energy. Good acceleration can be obtained over an r.f. pulse starting time range of 5 microseconds and frequency range of 0.5 megacycle.

BIBLIOGRAPHY

(1) V. I. Veksler, Journal of Physics (U.S.S.R.), Vol. 9, 153 (1945).

(2) E. M. McMillan, Physical Review, Vol. 68, 142 (1945).

(3) H. C. Pollock, Physical Review, Vol. 69, 125 (1946).

(4) F. K. Goward and D. E. Barnes, Nature, Vol. 158, 413 (1946).

(5) F. R. Elder, A. M. Gurewitsch, R. V. Langmuir and H. C. Pollock, Journal of Applied Physics, Vol. 18, 810 (1947).

(6) A. M. Gurewitsch, General Electric Company Data Folder No. 74735 dated August 12, 1947.

(7) D. W. Kerst and R. Serber, Physical Review, Vol 60, 53 (1941).

(8) D. Bohm and L. Foldy, Physical Review, Vol. 70, 249 (1946).

(9) "Handbook for the Users of Hanovia Bright Gold," Prepared by W. Riehl, Manager of the Ceramic Division of Hanovia Chemical and Mfg. Co. (1946).

(10) A. C. Helmholz, J. V. Franck and J. M. Peterson, "Synchrotron Radio Frequency System," U. S. Atomic Energy Commission Document MDDC 151, June 17, 1946.

(11) F. E. Terman, "Radio Engineers Handbook," McGraw-Hill Book Co., 1943.

(12) W. Abson and L. S. Holmes, A. E. R. E. Report G/R 192, May 5, 1948 (Great Britain).

(13) J. P. Blewett, Physical Review, Vol. 69, 87 (1946).

(14) L. Arzimovich and I. Pomeranchuk, Journal of Physics (U.S.S.R.), Vol. 9, 267 (1945).

Fig. 1 R.f. oscillator, coaxial stubs and accelerating grids for first synchrotron vacuum chamber, which consisted of a phenolic inner and outer ring sealed by rubber gaskets to the magnet pole tips.

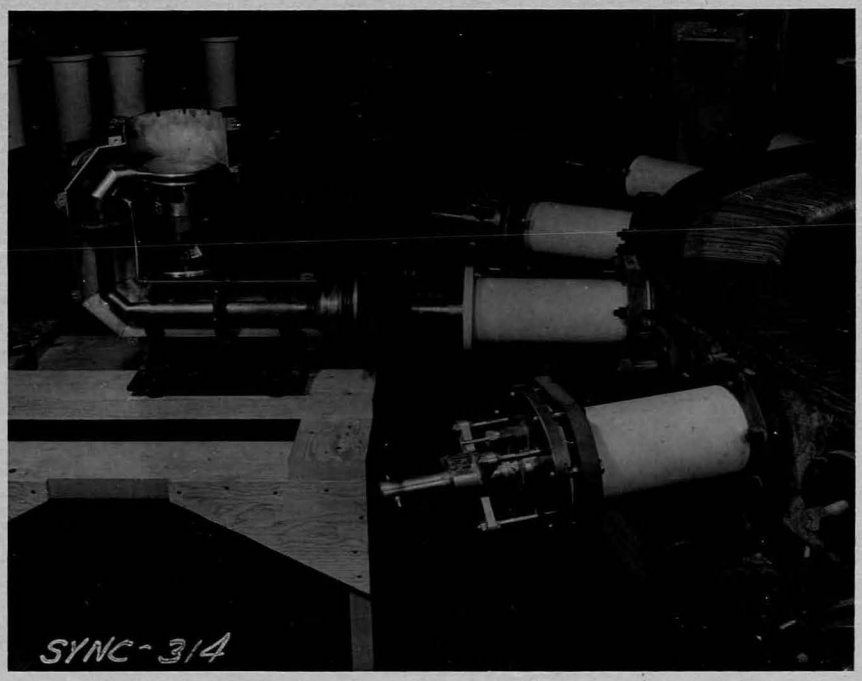

OZ 396

Fig. 2 End view of accelerating grids, showing beam aperture. The capacity of the coaxial grids was resonated at 47.7 mc by the inductive coaxial stubs attached to the phenolic ring. The voltage was uniform over the length of the C shaped 135° accelerator. Electrons were accelerated at entrance to the inner conductor and again at exit, the voltage having changed phase while the electron bunch traveled through the inner conductor drift space.

OZ 398

Fig. 3 The quartz vacuum chamber. The ends of the 45° segments are painted with glyptal to form a smooth surface and are sealed by rubber boots.

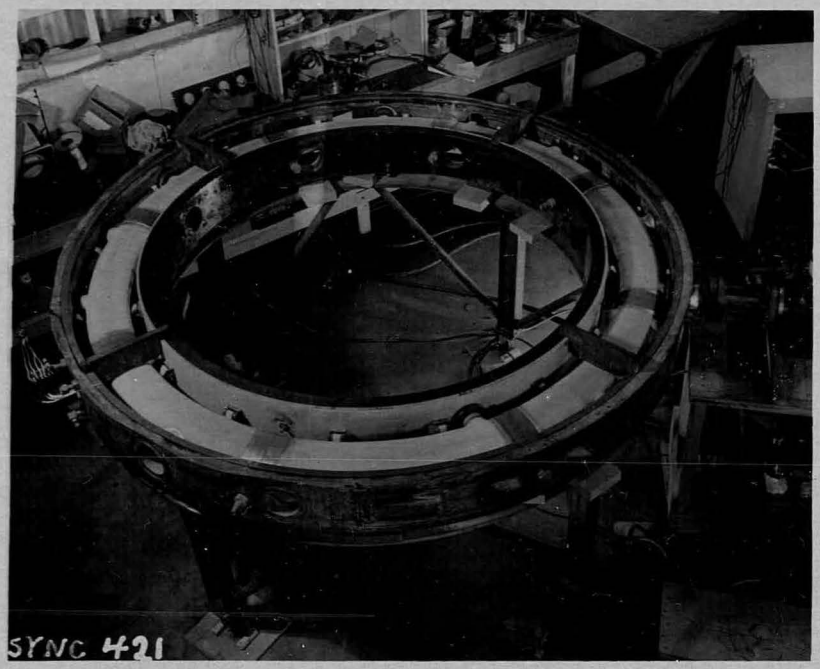

OZ 388

Fig. 4 Calculated curves of minimum r.f. voltage.

$E = 2\pi r H$

$H = \frac{3.77 \times 10^6}{6.28 \times 10^4}$

$\frac{3.8 \times 10^6}{6.2 \times 10^4 \times 10^{-8}}$

$\approx 2.8 \times 5 \times 10^2$ V

≈ 356

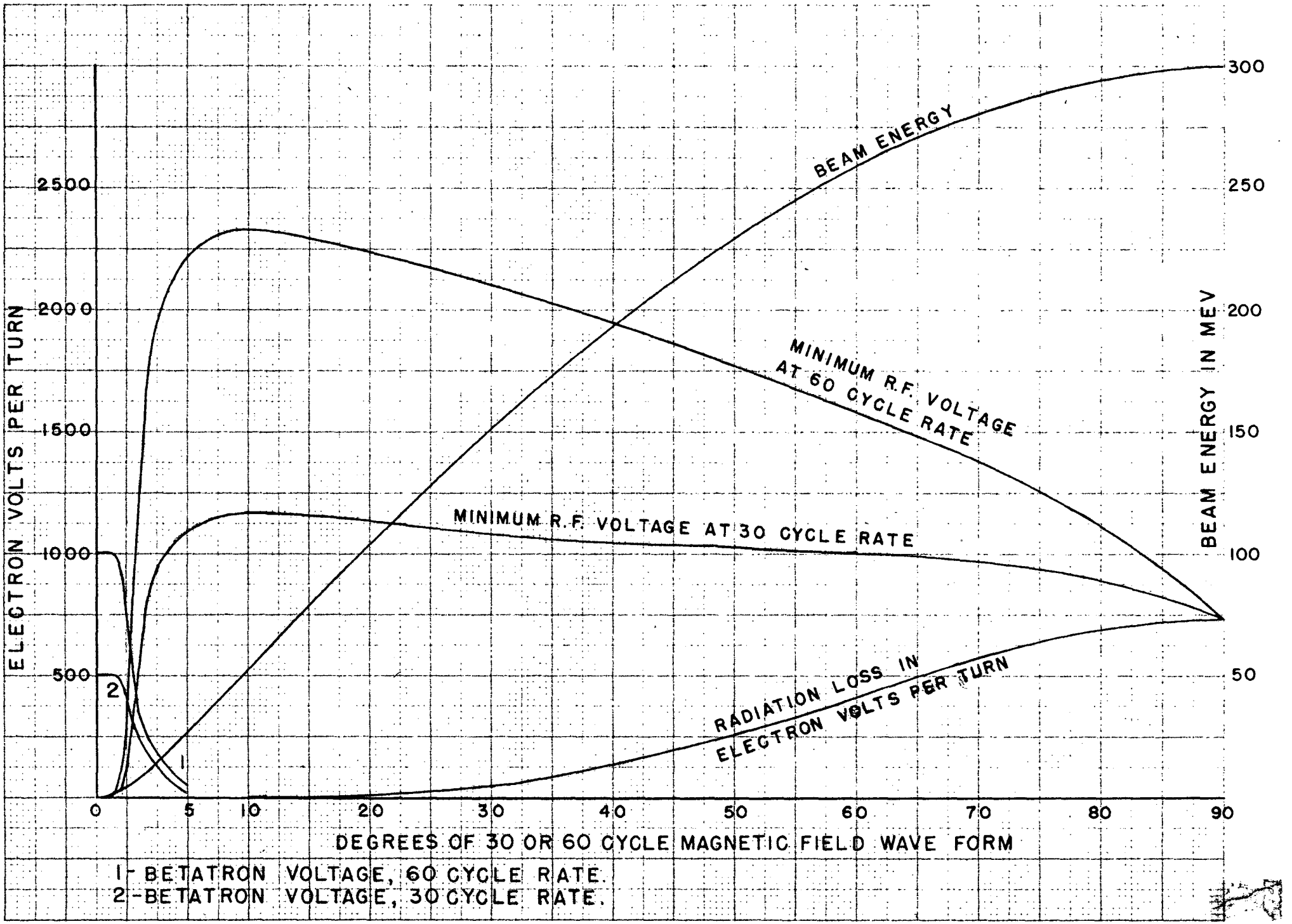
ELECTRON VOLTS PER TURN
2500
2000
1500
1000
500
BEAM ENERGY IN MEV
300
250
200
150
100
50
BEAM ENERGY
MINIMUM R.F. VOLTAGE AT 60 CYCLE RATE
MINIMUM R.F. VOLTAGE AT 30 CYCLE RATE
RADIATION LOSS IN ELECTRON VOLTS PER TURN
2
1
0
5
10
20
30
40
50
60
70
80
90
DEGREES OF 30 OR 60 CYCLE MAGNETIC FIELD WAVE FORM
1- BETATRON VOLTAGE, 60 CYCLE RATE.
2-BETATRON VOLTAGE, 30 CYCLE RATE.

13653-1

Fig. 5(a) View showing one of loops enclosing vertical field when scribe lines are not vertically arranged.

Fig. 5(b) Elementary loop of a long thin strip.

Fig. 5(c) Point displaced from center-line of long thin strip.

Fig. 5(d) Approximation of side strips.

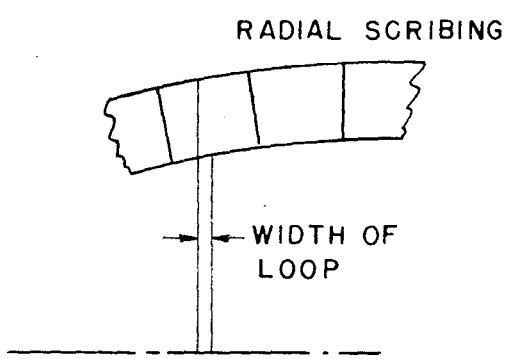

FIG. 5 (a)

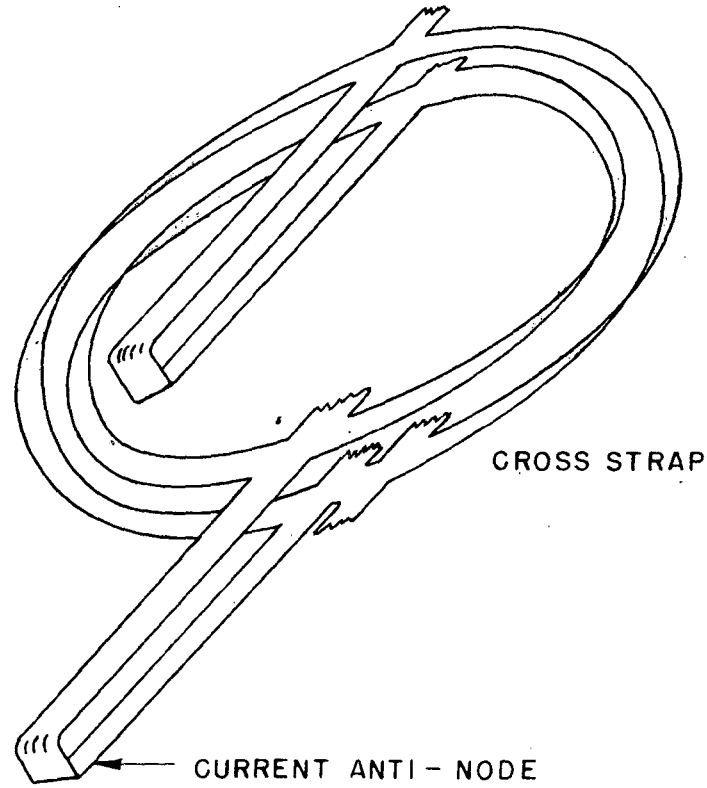

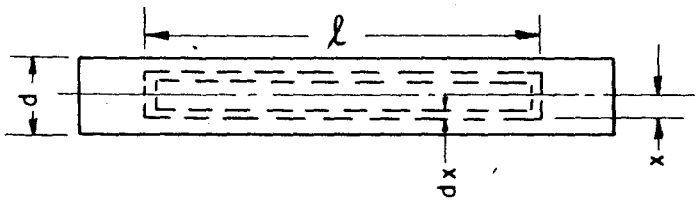

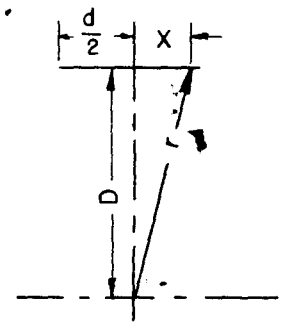

FIG. 5 (b)

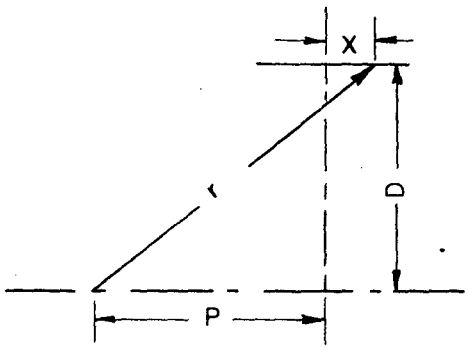

FIG. 5 (c)

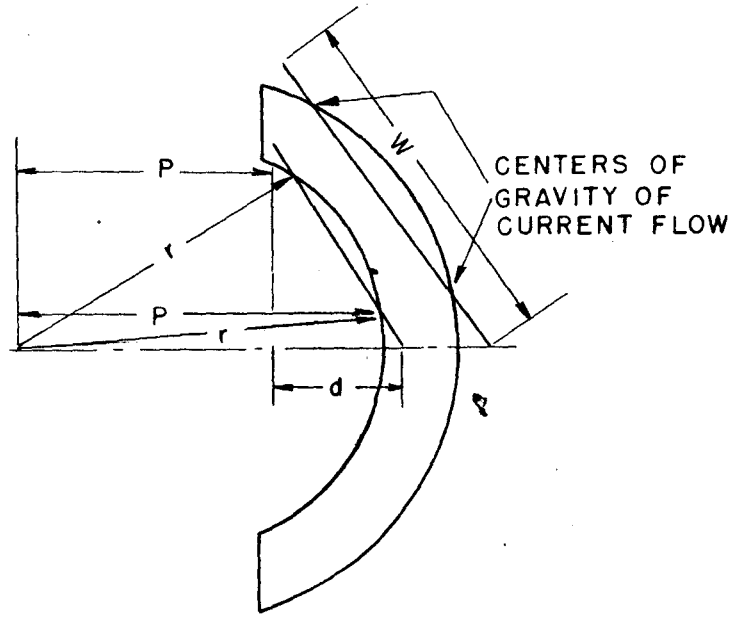

FIG. 5 (d)

Fig. 6 Calculated eddy current fields of vertically scribed resonator #1.

Solid lines are for 10 scribe lines top and bottom spaced 1.1 cm apart. See Fig. 16.

Broken lines are for 12 scribe lines top and bottom spaced 1.1 cm apart.

⊗ - means <u>measured</u> values of eddy current field.

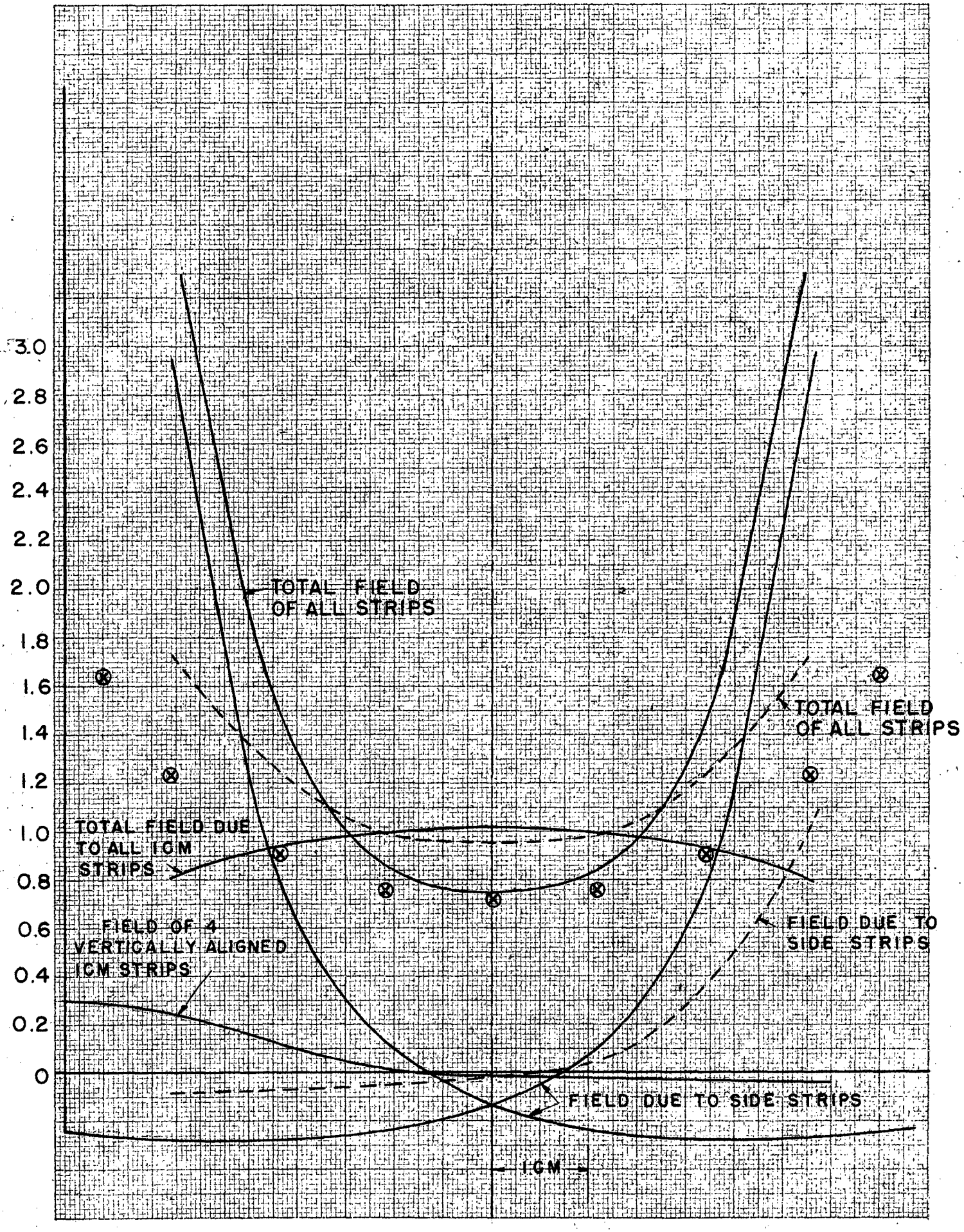

KEUFFEL & ESSER CO., N. Y. NO. 359-14 G
Millimeters, 5 mm. lines accented, cent. lines heavy.
MADE IN U.S.A.

13655-1

Fig. 7 Equipment used for measuring Q

A Pickup loop and 1N21 Crystal Rectifier

B D.c. galvanometer, shielded

C 35 GT shielded oscillator

D Power supply for oscillator.

E Frequency meter with crystal calibration.

F Oscilloscope for frequency meter output.

OZ 385

Fig. 8 Quartz resonator between pole tip wedges, with experimental zircon transformer in transmission line.

OZ 391

Fig. 9 Twice size air dielectric sheet copper replica of Quartz resonator, outside conductor opened.

OZ 400

Fig. 10 Twice size air dielectric sheet copper replica of quartz resonator for determination of current flow lines in surface.

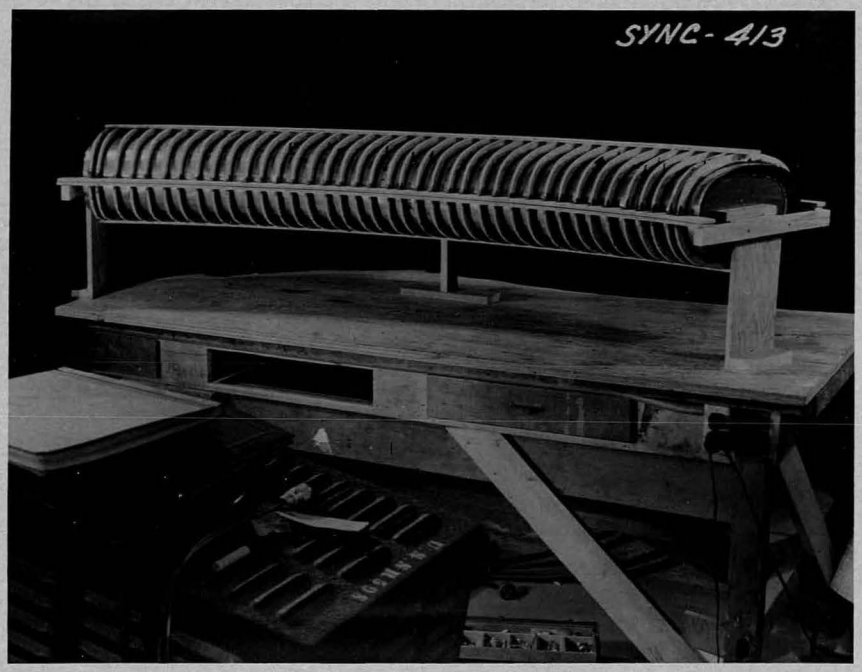

OZ 399

FIG. 11

SMOOTHED PLOT OF CURRENT FLOW LINES
IN
UNSCRIBED SHEET COPPER MODEL OF QUARTZ RESONATOR

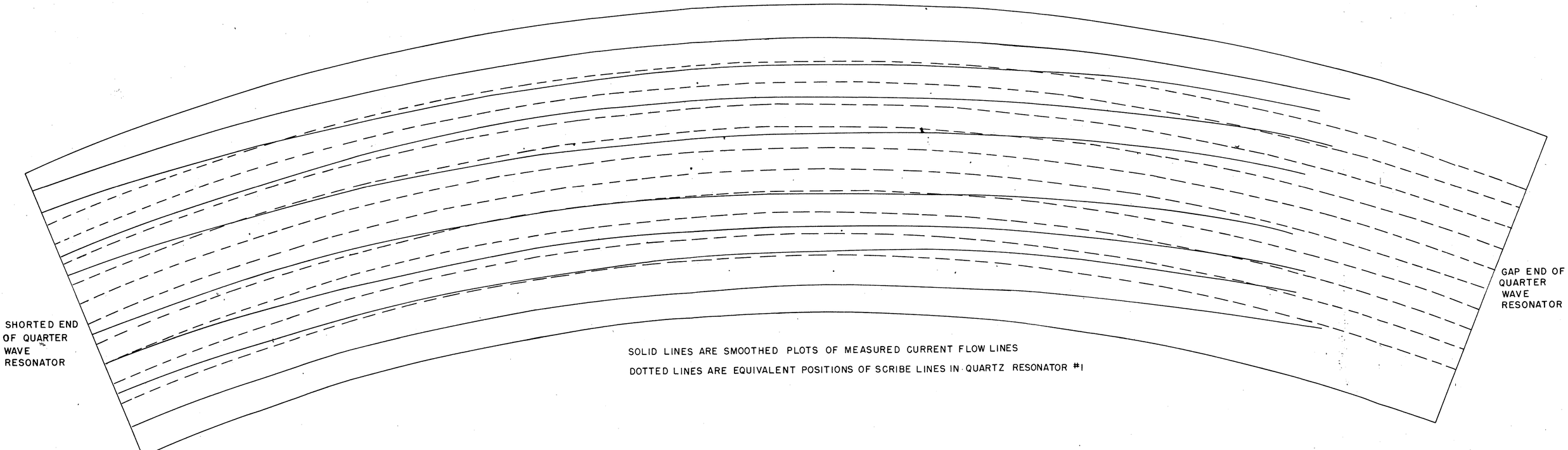

Fig. 12 Quartz resonator, showing some of the cross-strap positions for Q measurements.

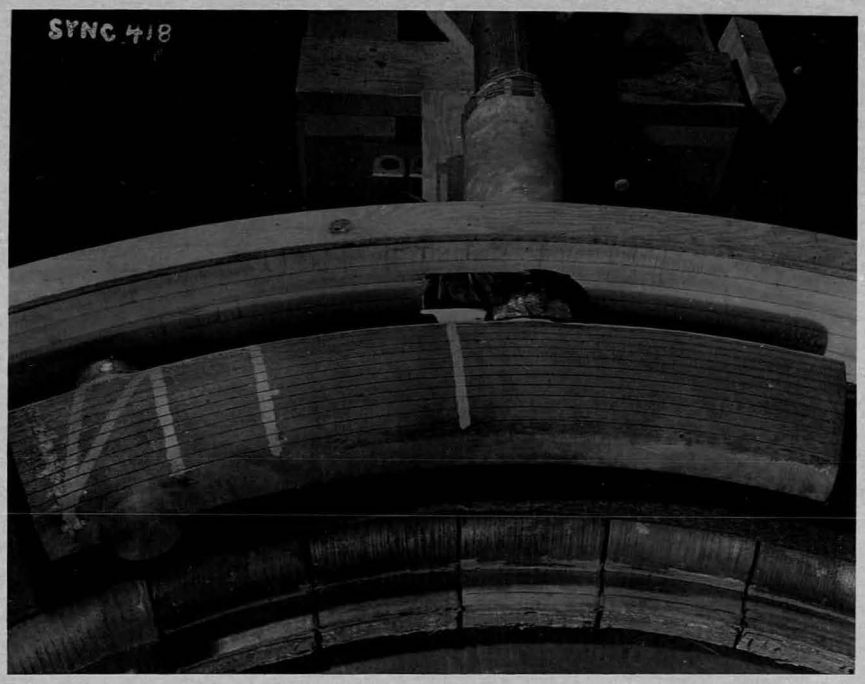

OZ 394

Fig. 13 Table of Q measurements

Distance from gap to cross-strap, measured along center-line	Q away from pole tips	Q between pole tips
1. Vertically scribed resonator #1.		
(a) Rough non-uniform outer surface. Air drying silver cross-strap:		
0 inches from gap	134	36
(Slanted, 0 to 1 3/4 inches)	178	44
4 inches from gap	233	52
8	259	63
15	252	145
(b) Outer surface smoothed and replated. Air drying silver cross-strap:		
0 inches from gap	138	---
10	226	127
13	320	191
15	242	155
19	160	125
30 (Current anti-node)	111	66
(c) Air drying silver cross-strap replaced with electroplated strap:		
13 inches from gap	342	225
2. Radially scribed resonator #2.		
(a) Air drying silver cross-strap		
0 inches from gap	409	234
7	448	318
13	490	360
(b) Electroplated cross-strap:		
13 inches from gap	545	445

Fig. 14 Equipment for measuring eddy current magnetic field.

A GL414 thyratron controlled exciter for energizing magnet.

B Flux bars from synchrotron.

C Pole tip wedges.

D Peaking strip for measuring phase of magnetic field.

E Peaking strip used to trigger synchroscope and exciter.

F Synchroscope.

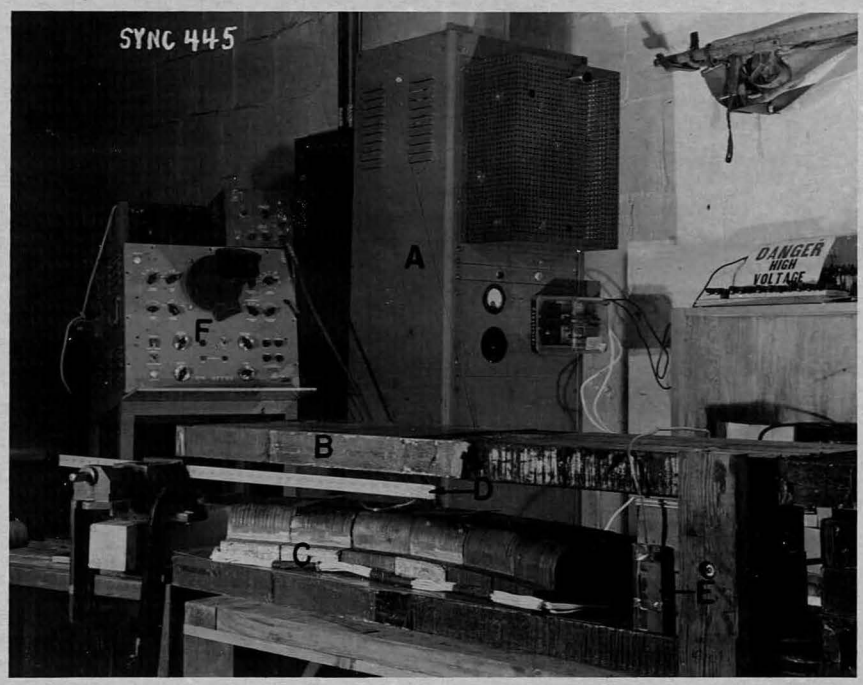
SYNC 445
A
B
C
D
E
F
DANGER
HIGH
VOLTAGE

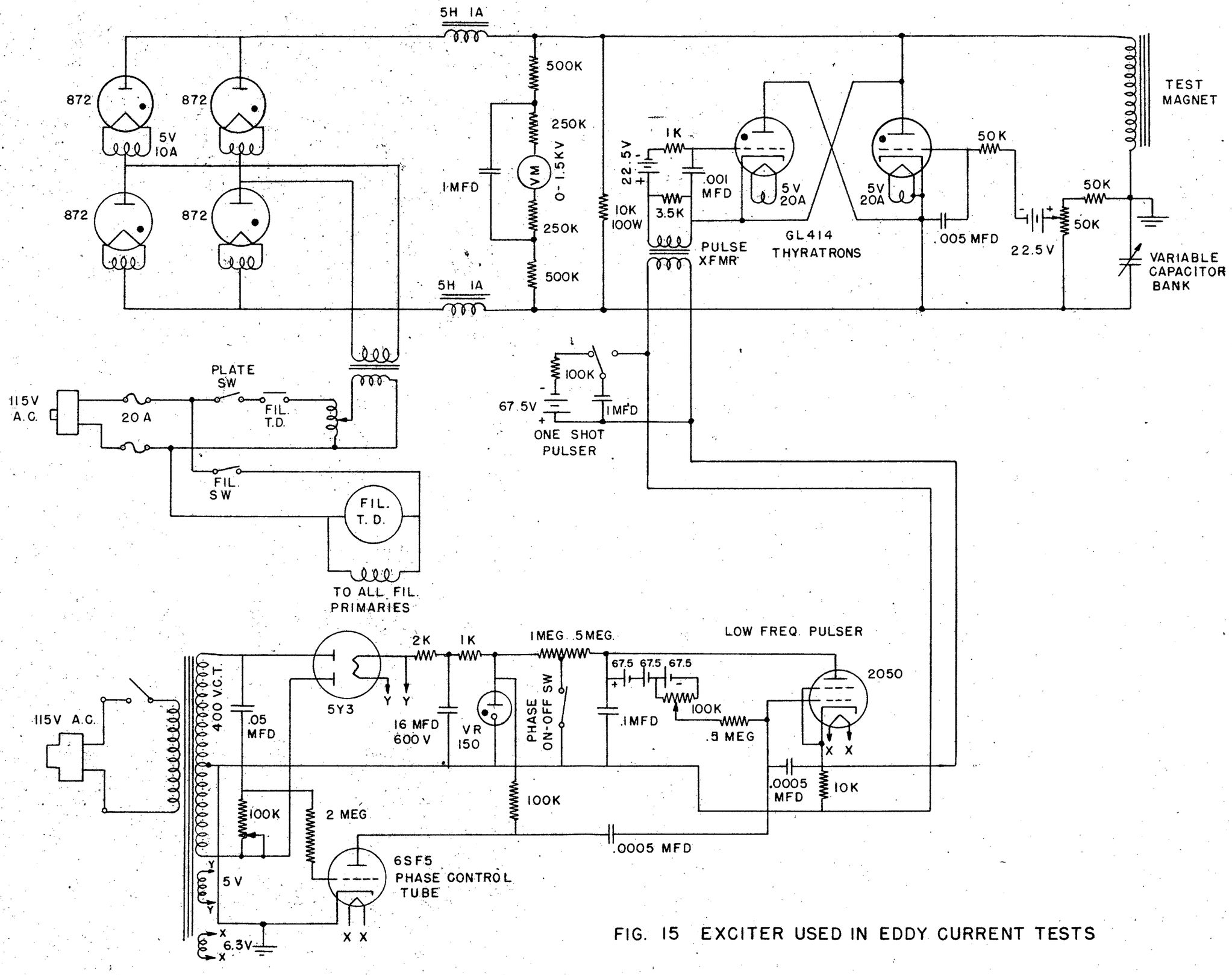

FIG. 15 EXCITER USED IN EDDY CURRENT TESTS

Fig. 16 Eddy current fields of quartz resonator #1.

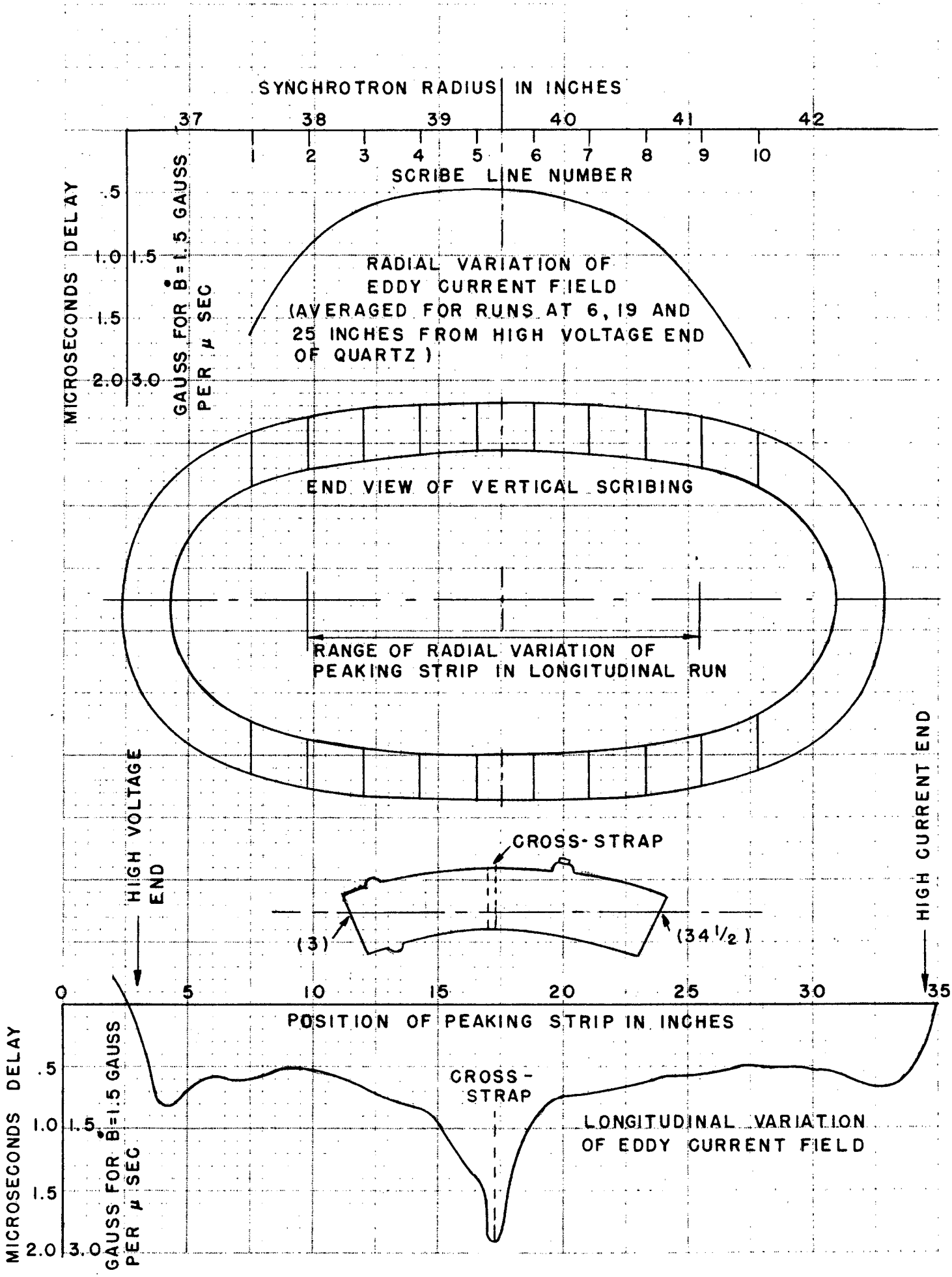

13657-1

PRINTED IN U.S.A. ON CLEARPRINT TECHNICAL PAPER NO 1000H
TECHNICHART
T35 10 X 10 DIVISIONS PER INCH 70 X 100 DIVISIONS
CLEARPRINT PAPER CO.

Fig. 17 Eddy current fields of quartz resonator # 2.

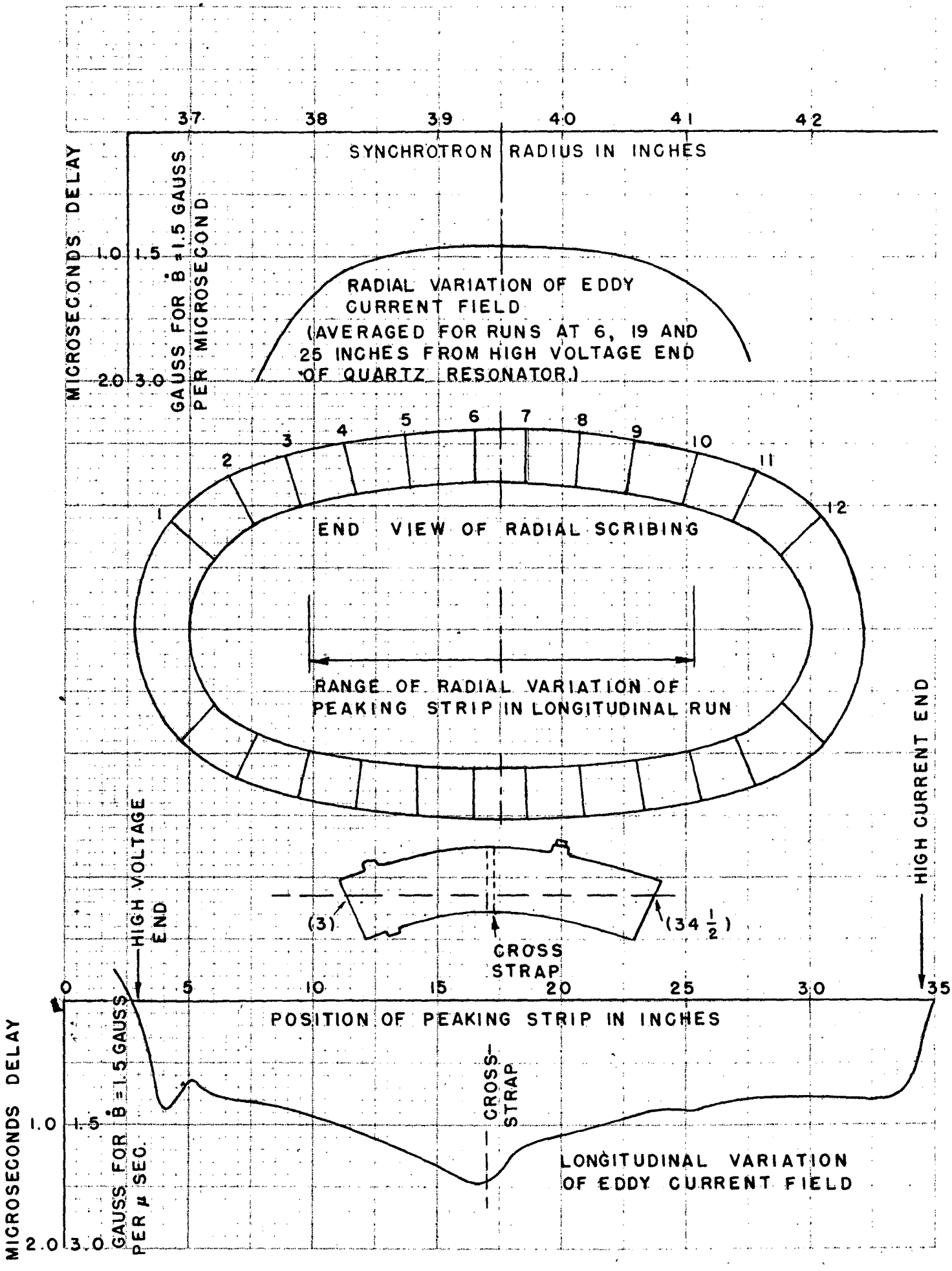

PRINTED IN U.S.A. ON CLEARPRINT TECHNICAL
TECHNI-CHART
CLEARPRINT PAPER CO. T35 10 X 10 DIVISIONS PER INCH 70 X 100 DIVISIONS

FIG. 18 PULSER FOR R.F. OSCILLATOR

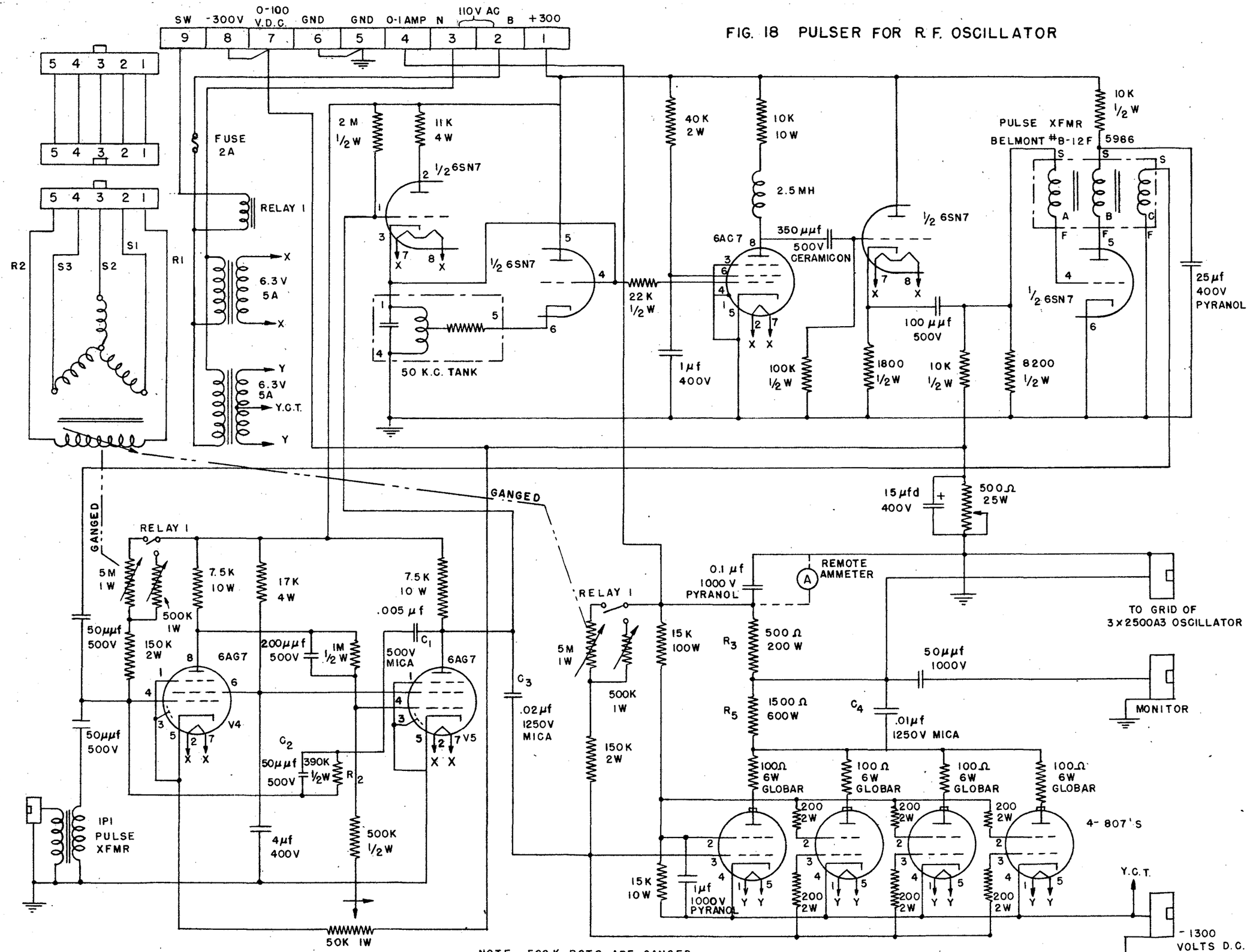

NOTE 500 K POTS ARE GANGED.
ALL TUBE SHIELDS ARE GROUNDED

Fig. 19 Schematic diagram of 3 X 2500 A3 r.f. oscillator

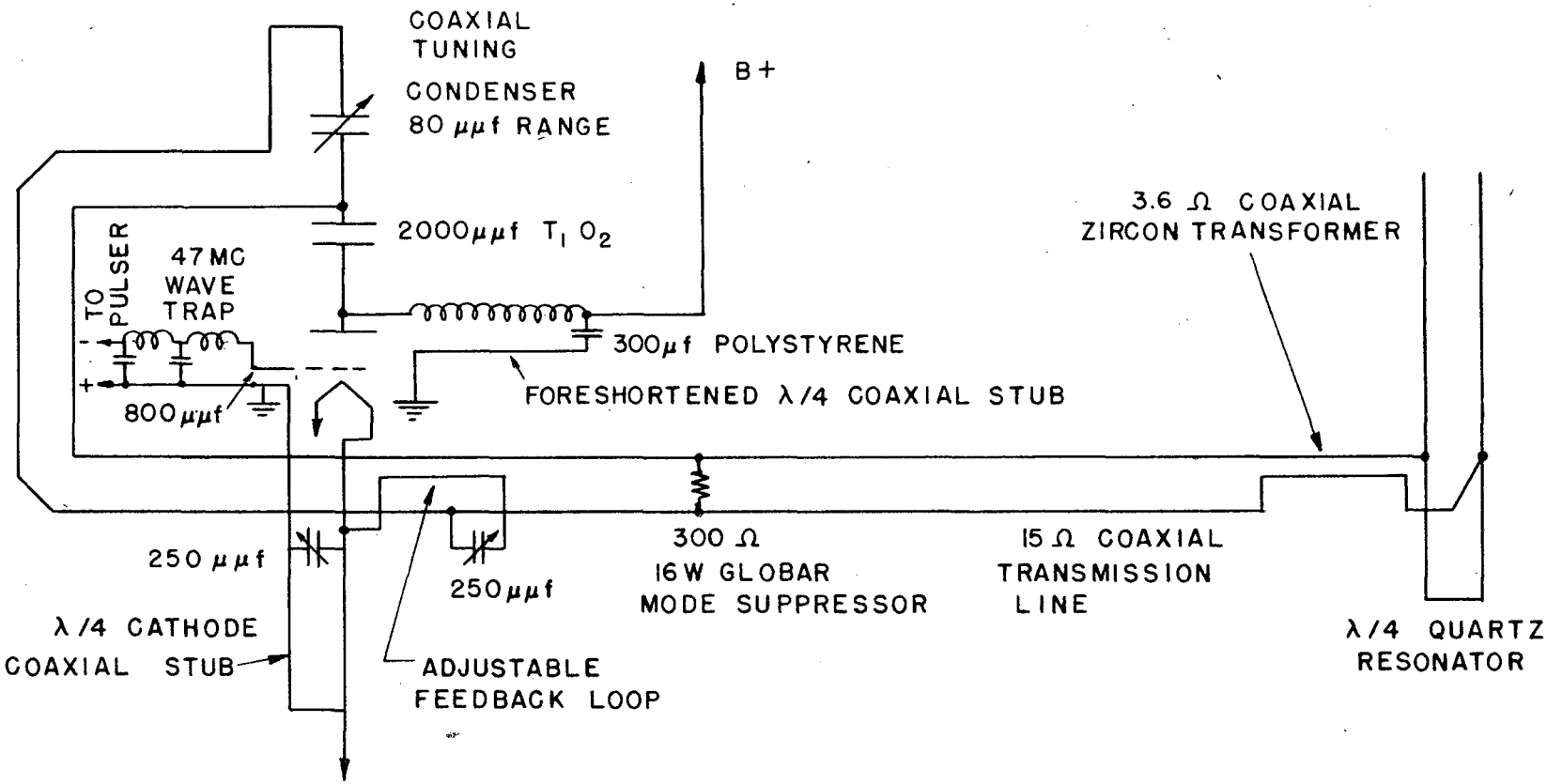
COAXIAL
TUNING
CONDENSER
80 μμf RANGE
B+
2000μμf $T_1 O_2$
3.6 Ω COAXIAL
ZIRCON TRANSFORMER
TO PULSER
47 MC
WAVE
TRAP
300μf POLYSTYRENE
FORESHORTENED λ/4 COAXIAL STUB
800μμf
250 μμf
250μμf
300 Ω
16W GLOBAR
MODE SUPPRESSOR
15 Ω COAXIAL
TRANSMISSION
LINE
λ/4 CATHODE
COAXIAL STUB
ADJUSTABLE
FEEDBACK LOOP
λ/4 QUARTZ
RESONATOR

13661-1

Fig. 20 Calculated voltage standing wave on 105 inch transmission line of first test oscillator. (Quartz resonator frequency = 49.7 mc; no zircon transformer).

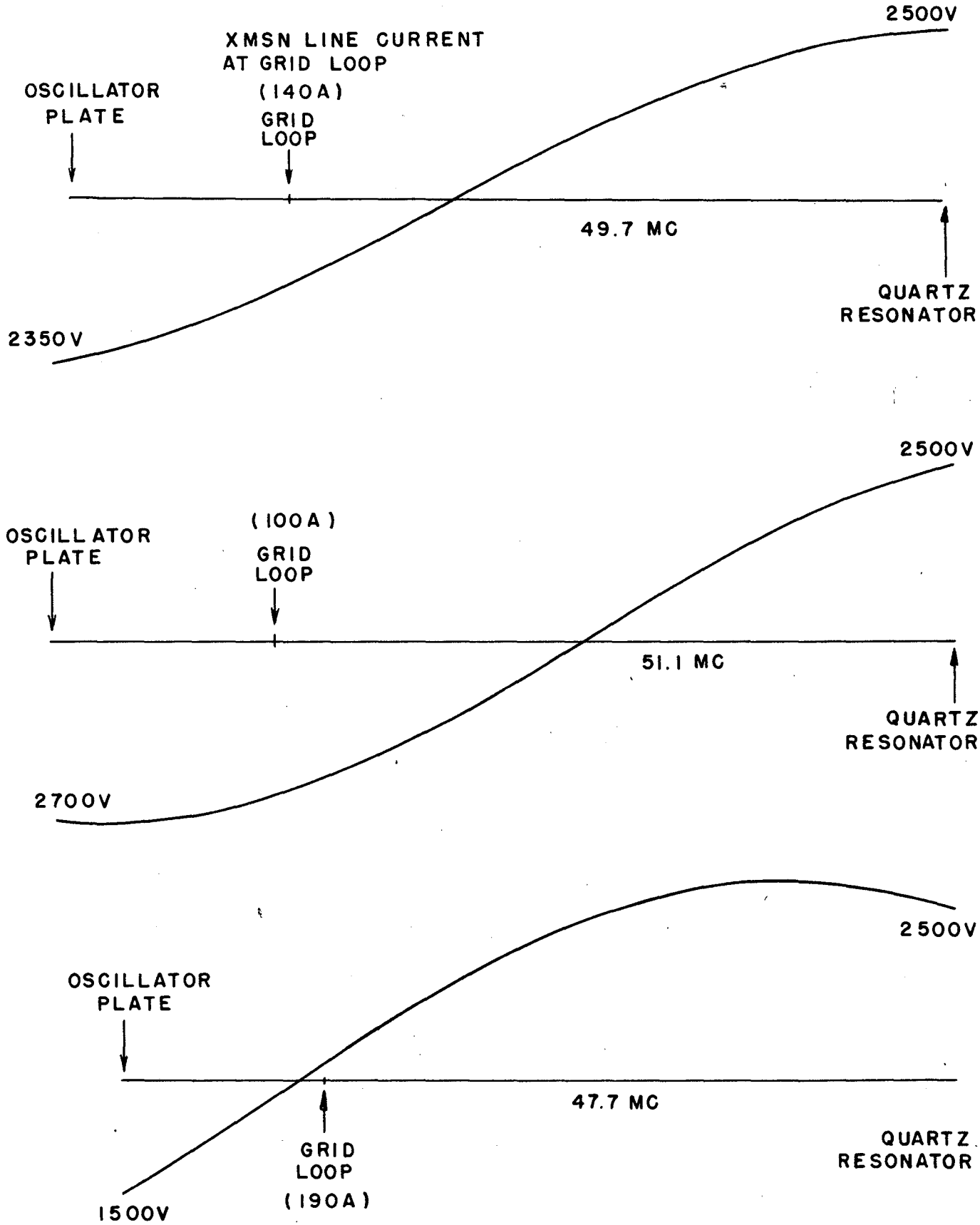
2500V
XMSN LINE CURRENT
AT GRID LOOP
(140A)
OSCILLATOR
PLATE
GRID
LOOP
49.7 MC
QUARTZ
RESONATOR
2350V
2500V
(100A)
OSCILLATOR
PLATE
GRID
LOOP
51.1 MC
QUARTZ
RESONATOR
2700V
2500V
OSCILLATOR
PLATE
47.7 MC
QUARTZ
RESONATOR
GRID
LOOP
(190A)
1500V

13662-1

Fig. 21 Calculated voltage standing wave on transmission line with zircon transformer. Quartz resonant at 49.7 mc.

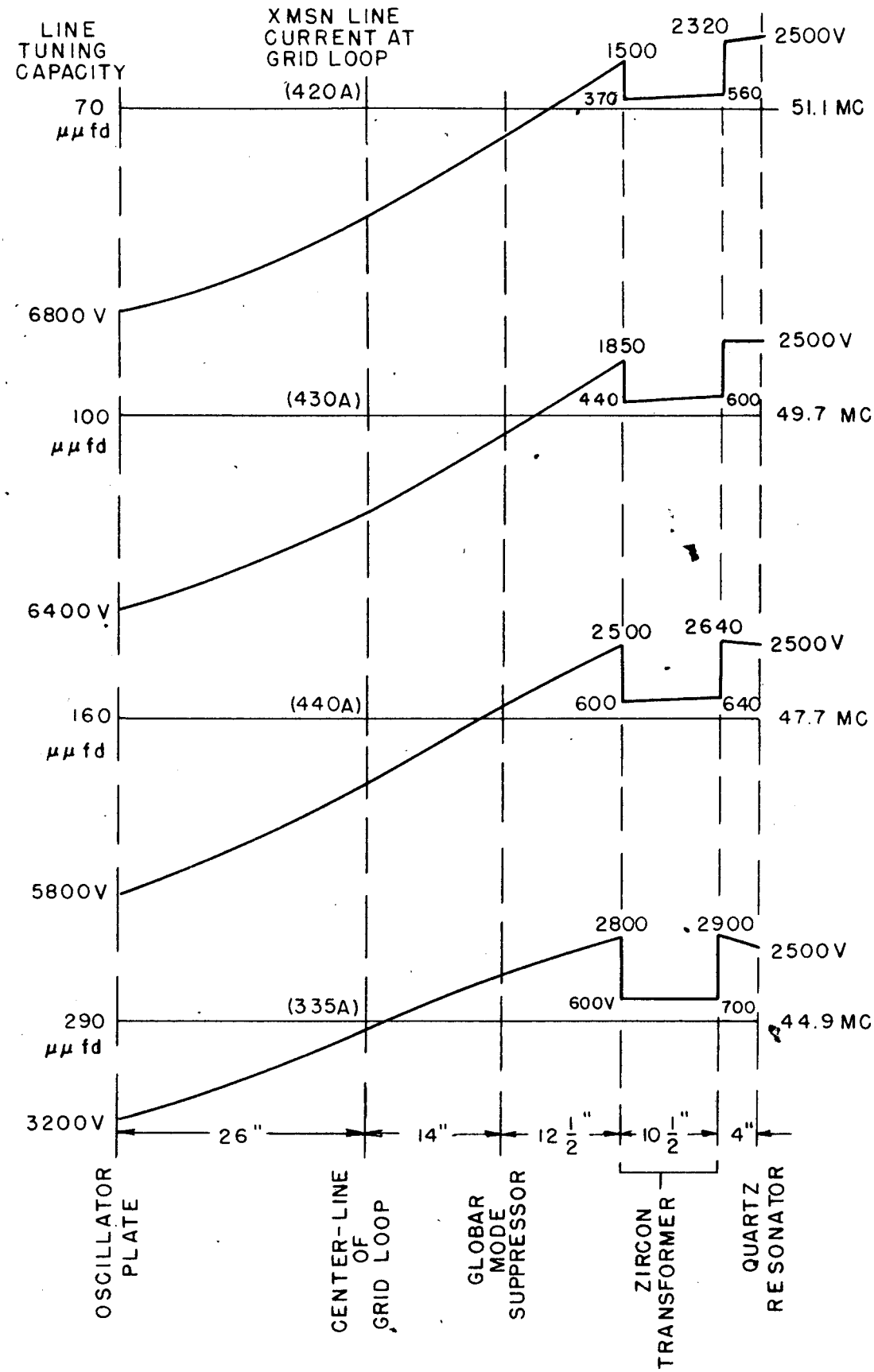
LINE TUNING CAPACITY
XMSN LINE CURRENT AT GRID LOOP
70 μμfd
(420A)
1500
370
2320
560
2500V
51.1 MC
6800 V
100 μμfd
(430A)
1850
440
2500V
600
49.7 MC
6400 V
160 μμfd
(440A)
2500
600
2640
640
2500V
47.7 MC
5800V
290 μμfd
(335A)
2800
600V
2900
700
2500V
44.9 MC
3200V
26"
14"
12 1/2"
10 1/2"
4"
OSCILLATOR PLATE
CENTER-LINE OF GRID LOOP
GLOBAR MODE SUPPRESSOR
ZIRCON TRANSFORMER
QUARTZ RESONATOR

13663-1

Fig. 22 Constant current characteristics of 3 X 2500 A3 triode.

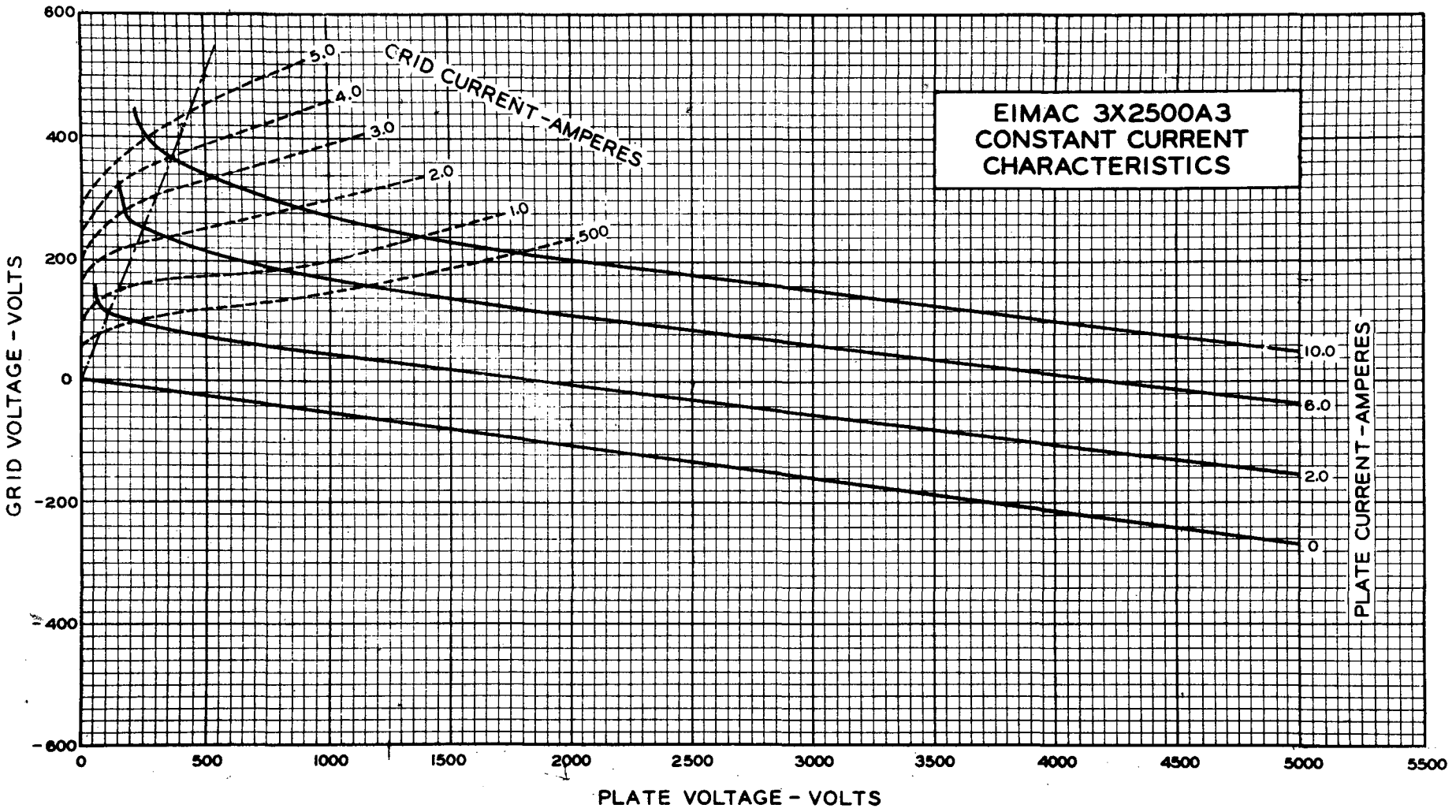
EIMAC 3X2500A3
CONSTANT CURRENT
CHARACTERISTICS
GRID CURRENT-AMPERES
5.0
4.0
3.0
2.0
1.0
.500
10.0
6.0
2.0
0
PLATE CURRENT-AMPERES
GRID VOLTAGE - VOLTS
600
400
200
0
-200
-400
-600
0
500
1000
1500
2000
2500
3000
3500
4000
4500
5000
5500
PLATE VOLTAGE - VOLTS

OZ. 430

Fig. 23 Oscillator operating voltages and currents.

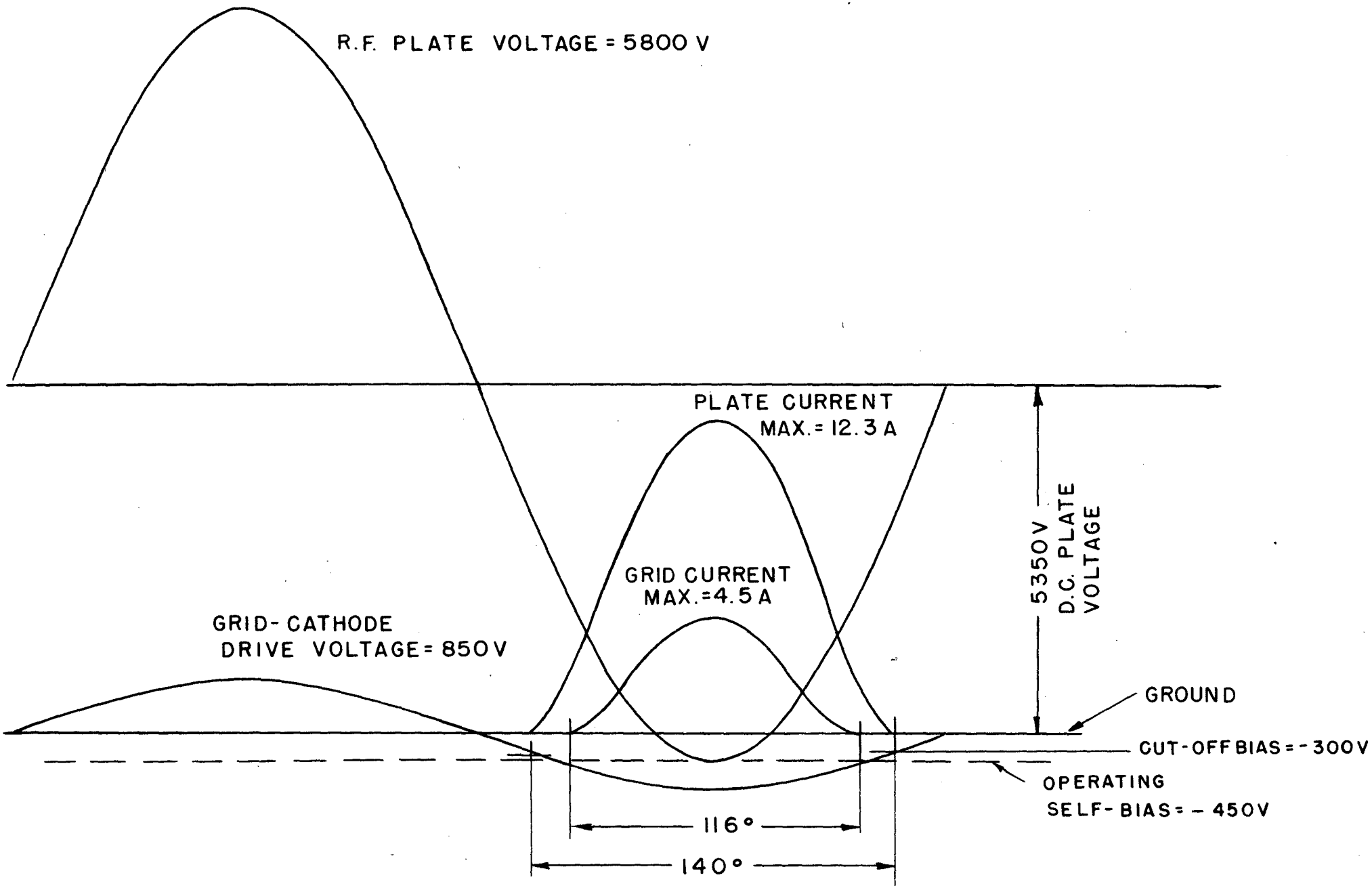
R.F. PLATE VOLTAGE = 5800 V
PLATE CURRENT
MAX. = 12.3 A
GRID CURRENT
MAX. = 4.5 A
GRID-CATHODE
DRIVE VOLTAGE = 850 V
5350 V
D.C. PLATE
VOLTAGE
GROUND
CUT-OFF BIAS = -300 V
OPERATING
SELF-BIAS = -450 V
116°
140°

13664-1

Fig. 24 R.f. test oscillator with zircon transformer.

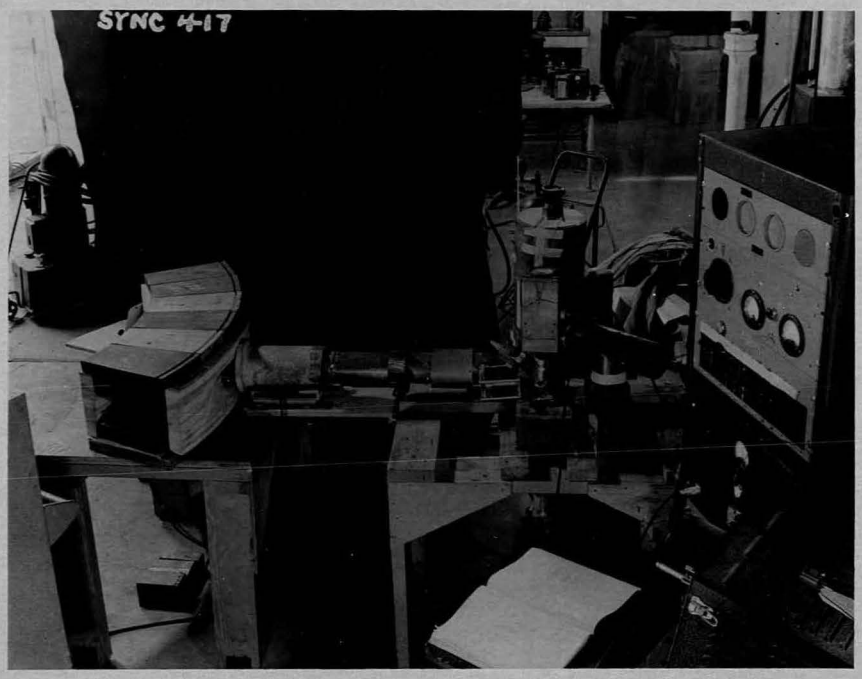
SYNC 417

Fig. 25 R.f. test oscillator and quartz resonator #1.

OZ 390

Fig. 26 Quartz resonator #2, showing radial scribing and feedpoint arrangement.

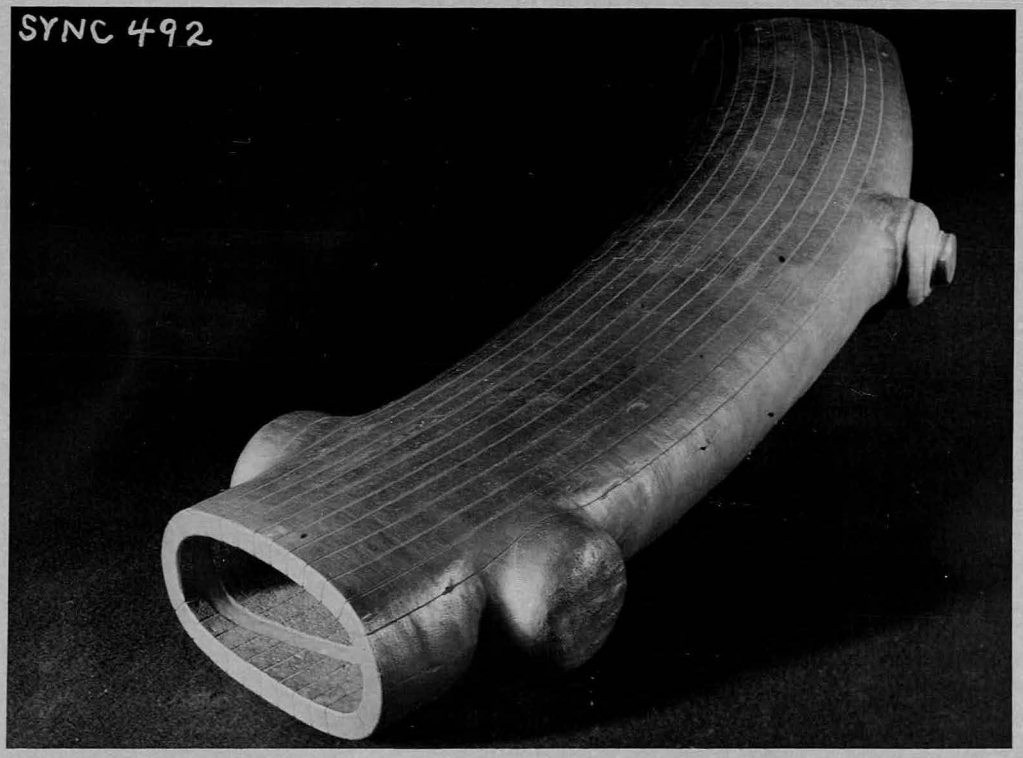

OZ.-429

Fig. 27 Final r.f. oscillator installed in synchrotron.

A Zircon transformer.

B Globar mode suppressor.

C Coupling loop tuning condenser.

D Cathode stem tuning condenser.

E Line tuning condenser, selsyn controlled.

F Tickler oscillator.

G Plate choke stub.

H Blower for cooling resonator.

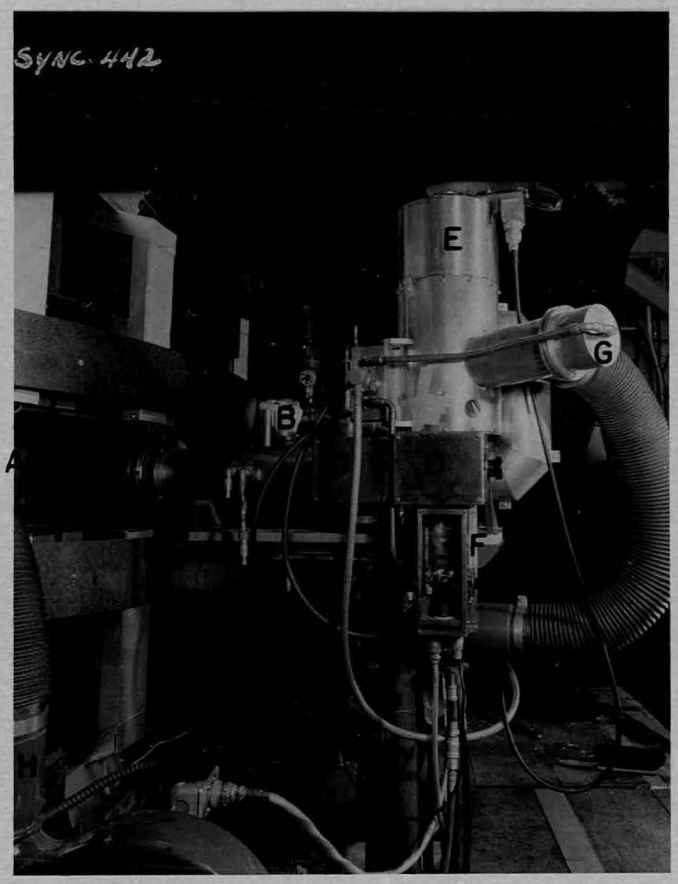

OZ 395

Fig. 28 Final r.f. oscillator.

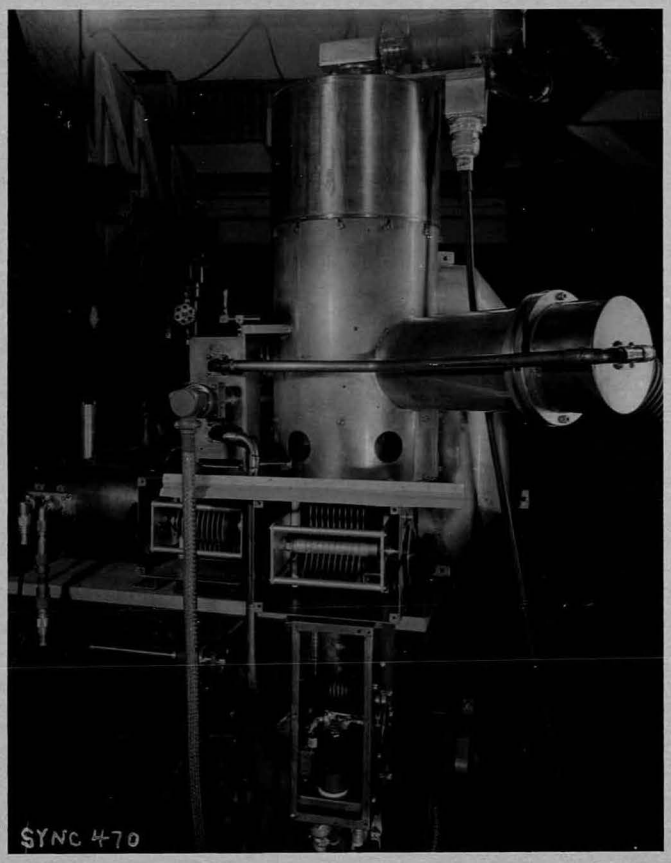

OZ 386

Fig. 29 Right side of final oscillator.

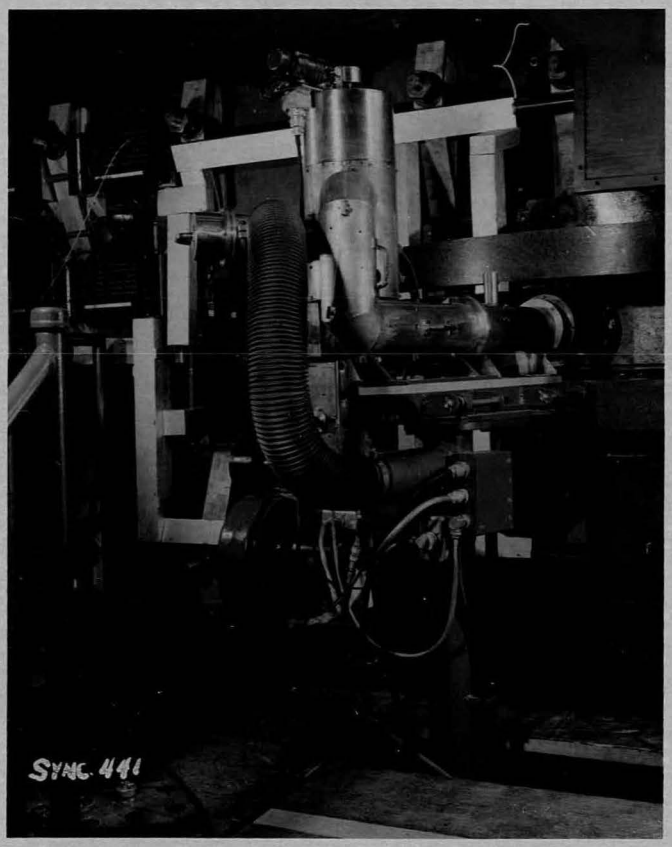

OZ 393

Fig. 30 Final oscillator with half of transmission line outer conductor removed. Note titanium dioxide disks which couple tube plate to line. Note polystyrene rods for setting feedback loop.

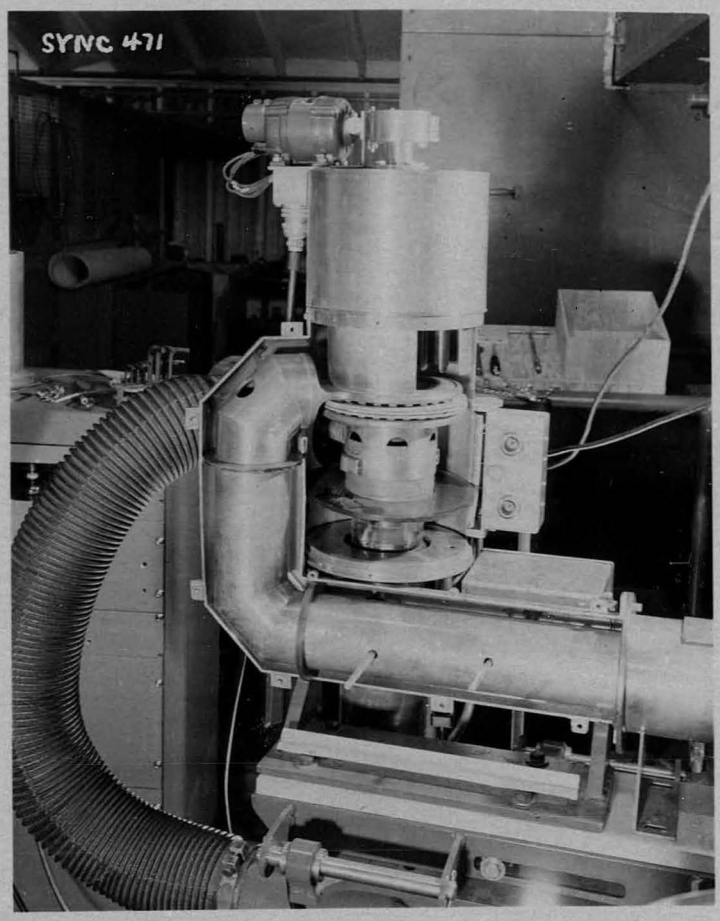

OZ 384

Fig. 31 Top view of oscillator installed in synchrotron.

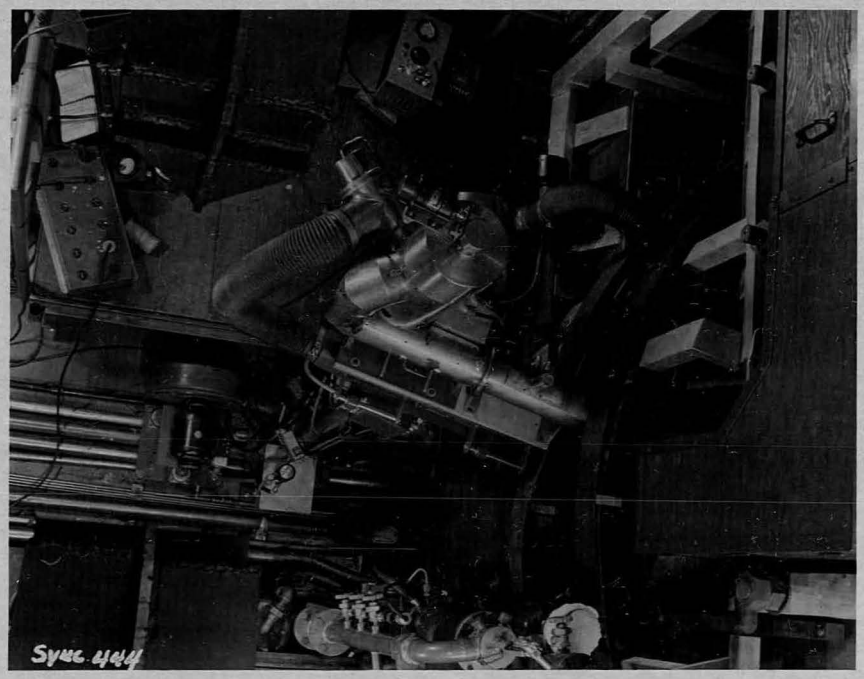

OZ 397

Fig. 32 Synchrotron beam intensity vs. oscillator frequency.

Notes:

(1) 300 Mev x-ray beam.

(2) Injector timed early to obtain constant intensity.

(3) R.f. pulse timing adjusted for maximum intensity at each frequency.

(4) Betatron signal 100 μ sec. after injection.

(5) Magnet frequency 30 cycle per second.

(6) R.f. voltage at quartz resonator gap = 2400 volts.

(7) .35 H choke in plate lead for pulse shaping.

CLEARPRINT PAPER CO. 135 10 X 10 DIVISIONS PER INCH 70 X 100 DIVISIONS
TECHNICHART
PRINTED IN U.S.A. ON CLEARPRINT TECHNICAL PAPER NO. 1000H

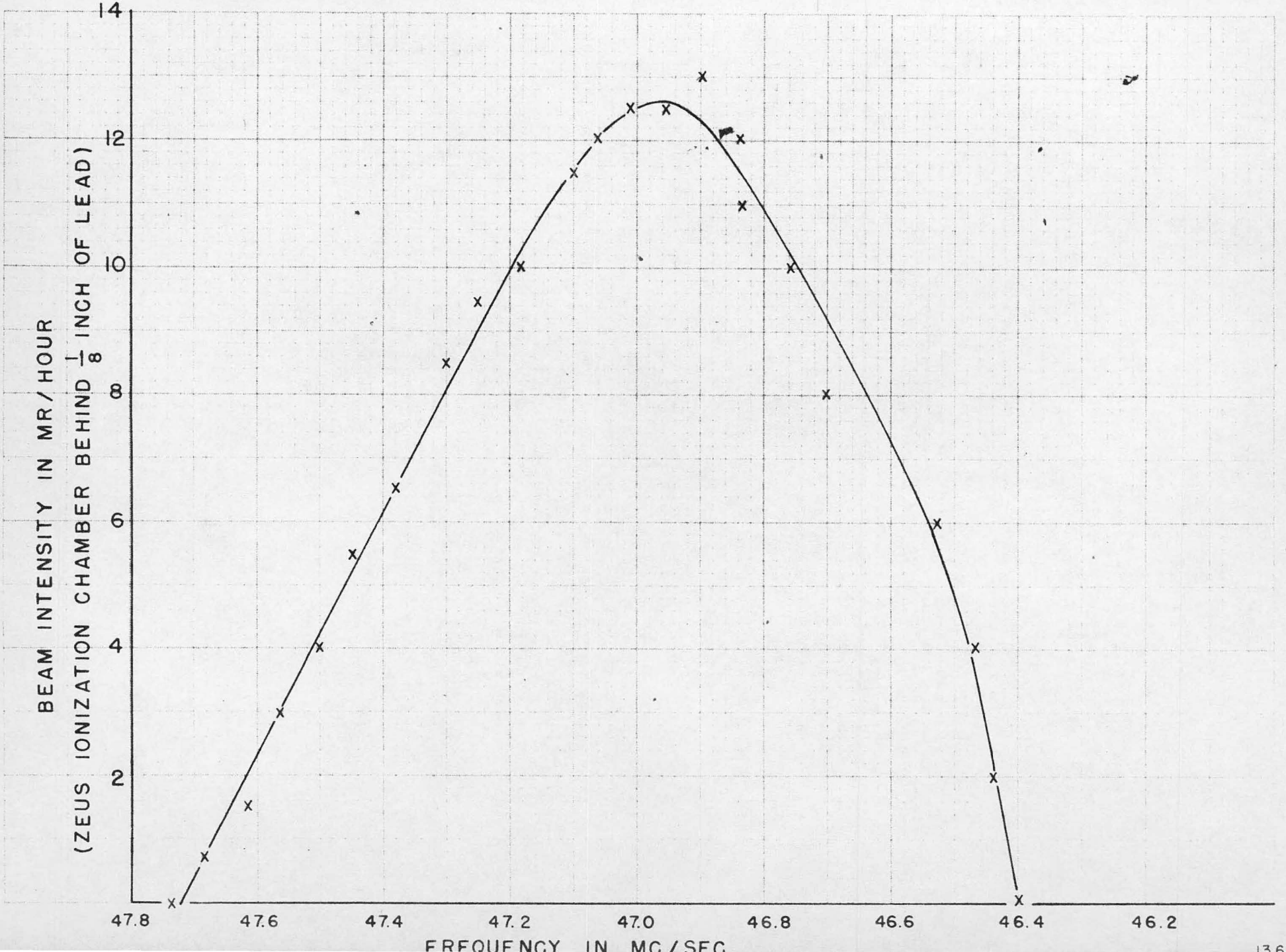

13665-1

Fig. 33 Synchrotron beam intensity vs. r.f. oscillator pulse turn-on time

Notes:

(1) 300 Mev x-ray beam.

(2) Injector timed early to obtain constant intensity. Beam about 30% of intensity obtained with optimum injector timing.

(3) R.f. voltage at quartz resonator gap = 2400 volts.

(4) .35 H choke in plate lead for pulse shaping.

(5) Magnet frequency = 30 cycles/second.

(6) Oscillator frequency = 46.9 mc/sec.

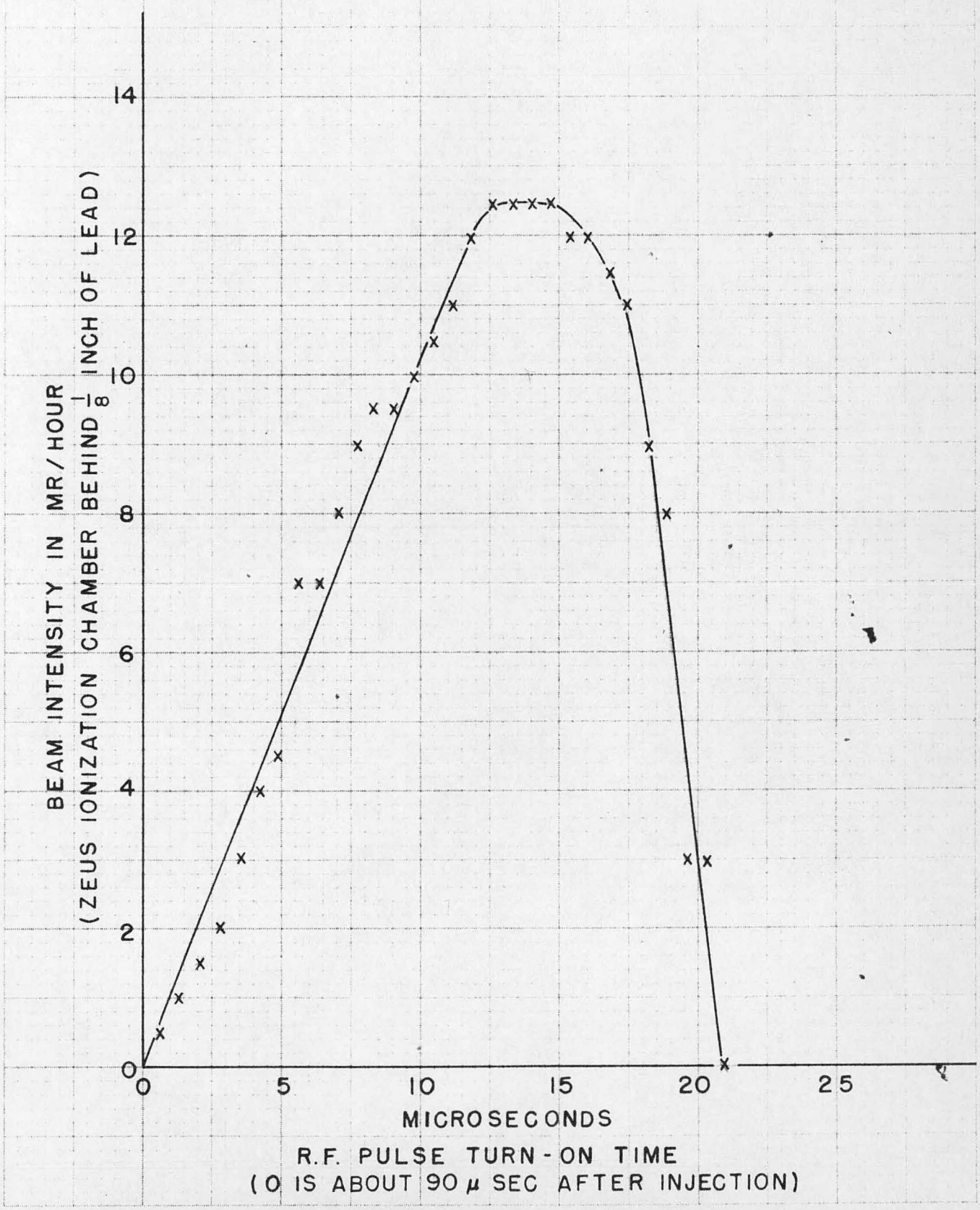

CLEARPRINT PAPER CO. T35 10 X 10 DIVISIONS PER INCH 70 X 100 DIVISIONS
PRINTED IN U.S.A. ON CLEARPRINT TECHNICAL PAPER NO. 1000H
TECHNICHART

Fig. 34 Synchrotron beam intensity vs. quartz resonator gap voltage.

(A) 7 μ sec. rise to full voltage. See Fig. 35(a)

(B) .35 H choke in plate lead of oscillator, producing 7 μ sec. rise to 30% and exponential rise to 100% voltage with 200 μ sec. time constant. See Fig. 35(b).

Notes:

(1) 300 Mev x-ray beam.

(2) Injector timed early to obtain constant intensity.

(3) Oscillator frequency = 46.9 mc/sec.

(4) Magnet frequency = 30 cycles/sec.

CLEARPRINT PAPER CO. T35 10 X 10 DIVISIONS PER INCH 70 X 100 DIVISIONS PRINTED IN U.S.A. ON CLEARPRINT TECHNICAL PAPER NO 1000H
TECHNICHART

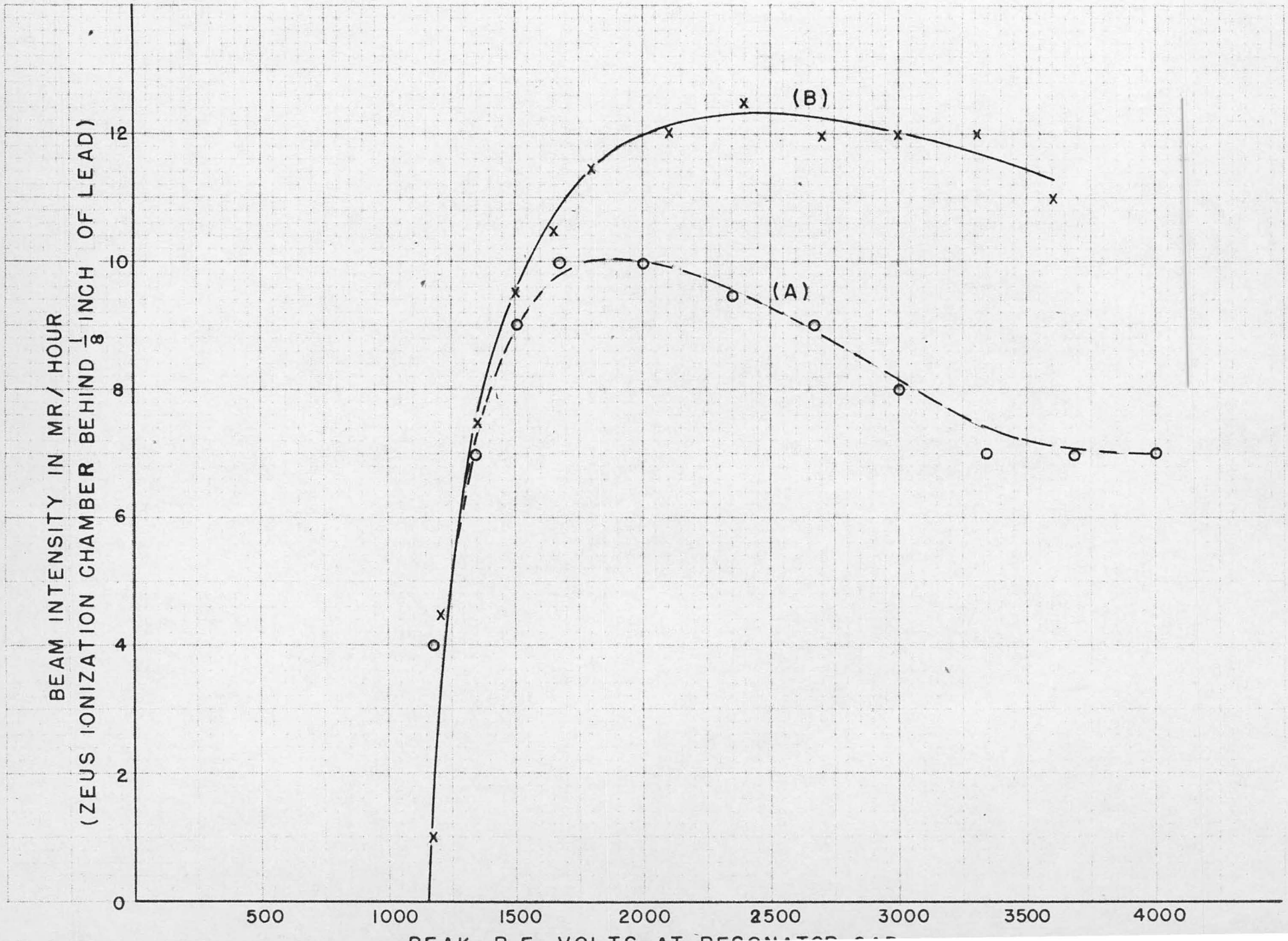

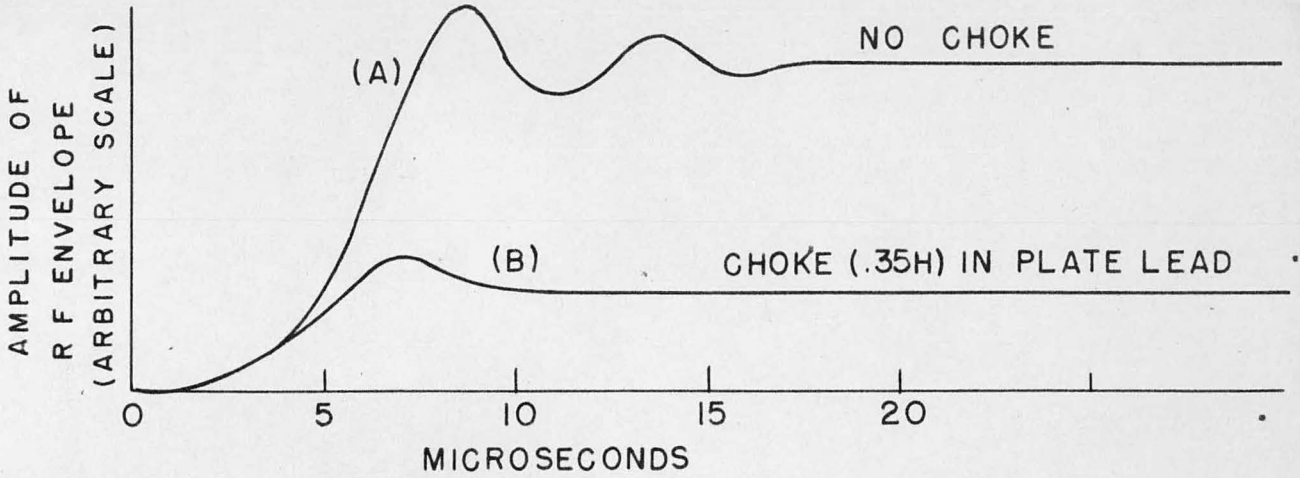
AMPLITUDE OF
R F ENVELOPE
(ARBITRARY SCALE)
(A)
NO CHOKE
(B)
CHOKE (.35H) IN PLATE LEAD
0
5
10
15
20
MICROSECONDS

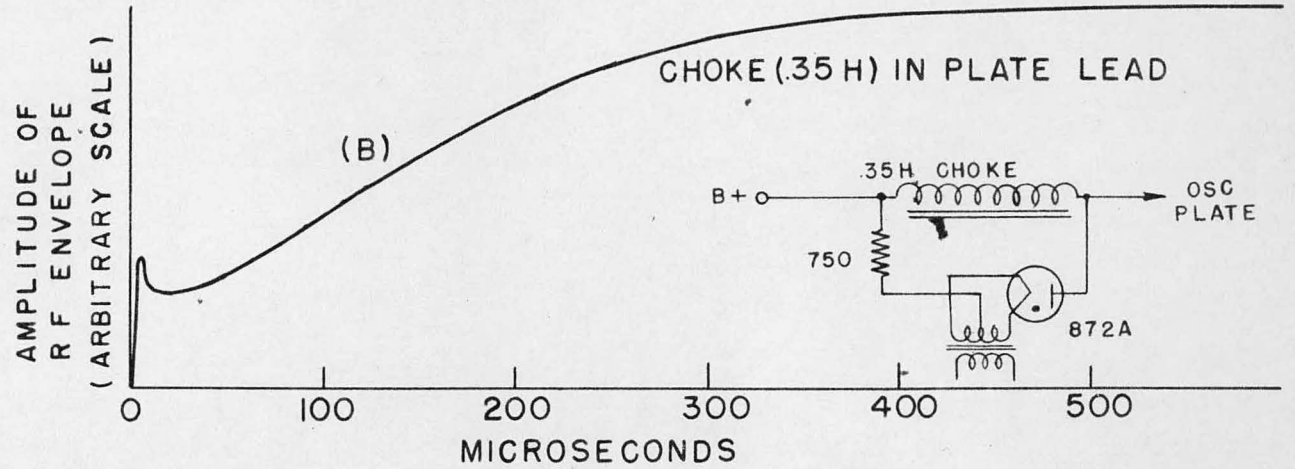
AMPLITUDE OF
R F ENVELOPE
(ARBITRARY SCALE)
CHOKE (.35 H) IN PLATE LEAD
(B)
.35H CHOKE
B+
OSC
PLATE
750
872A
0
100
200
300
400
500
MICROSECONDS

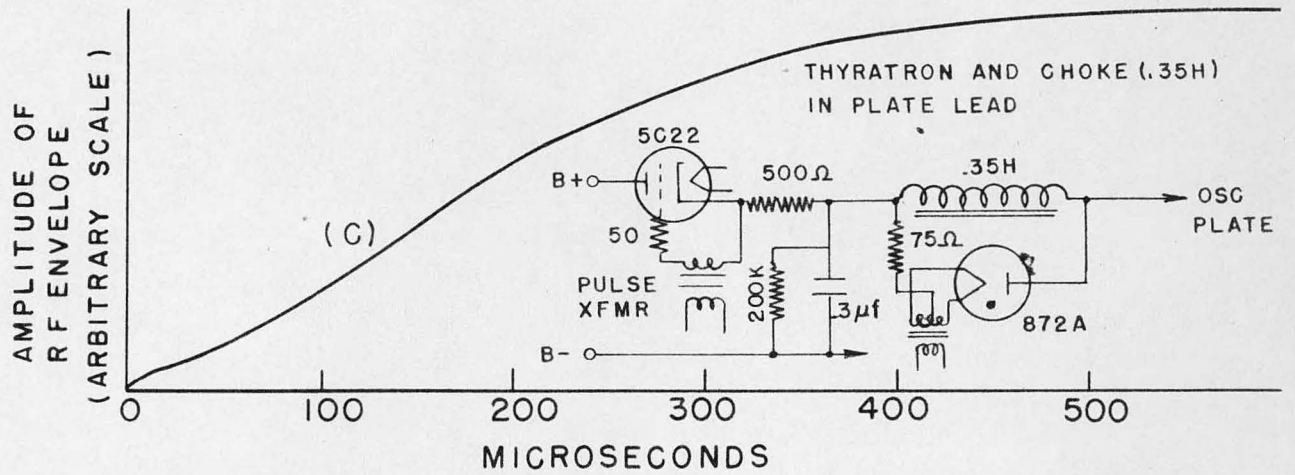
AMPLITUDE OF
R F ENVELOPE
(ARBITRARY SCALE)
THYRATRON AND CHOKE (.35H)
IN PLATE LEAD
5C22
B+
500Ω
.35H
OSC
PLATE
(C)
50
75Ω
PULSE
XFMR
200K
.3μf
872A
B-
0
100
200
300
400
500
MICROSECONDS

13668-1

Fig. 36 Synchrotron beam photograph.

1 inch

280 MeV X-rays
5 feet from target
1/17/49

OZ 389

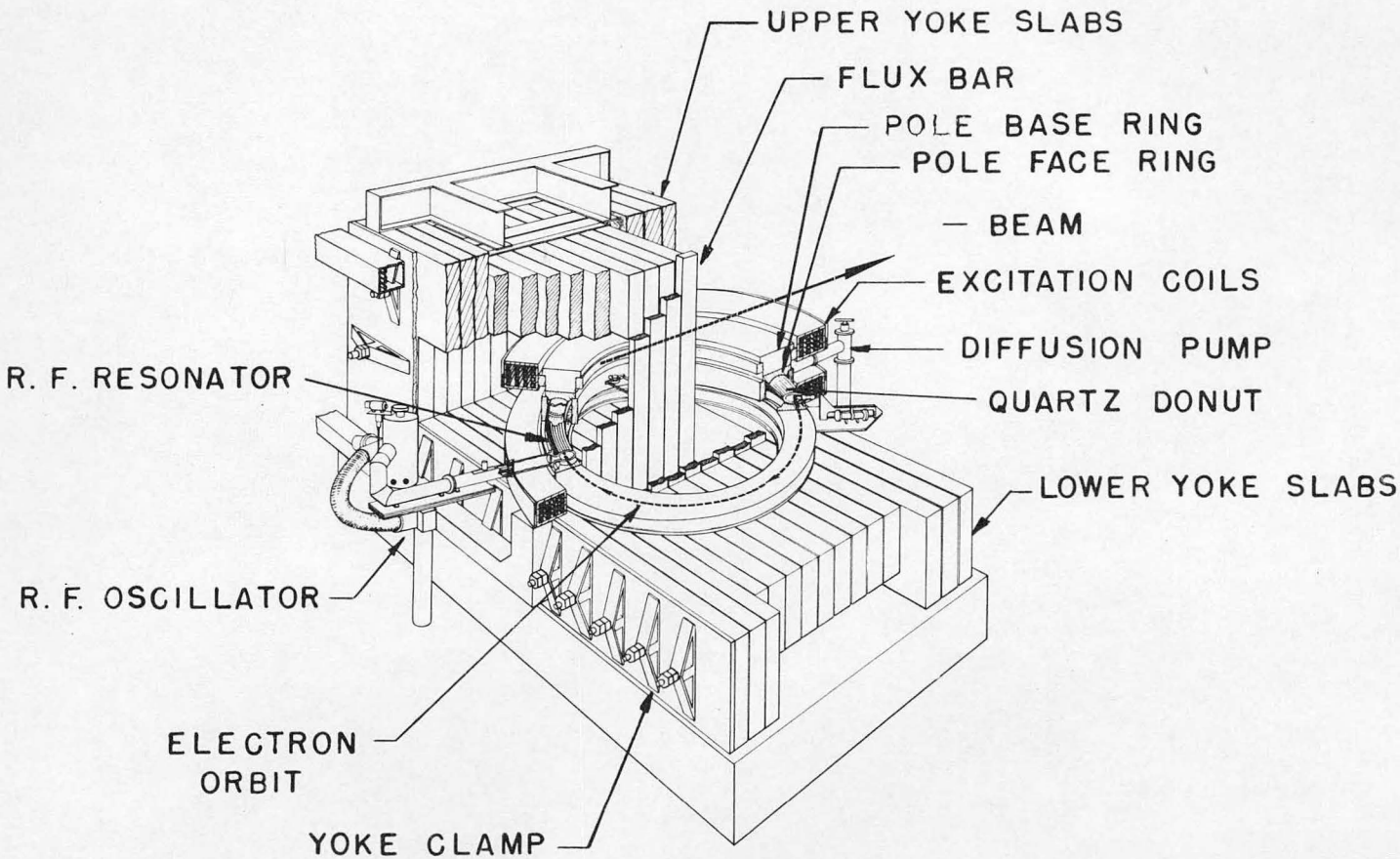

CUTAWAY VIEW OF SYNCHROTRON

FIG. 37

MATERIAL 4C8602B - R.F. SEGMENT MOLDING DETAIL

SHOWN ON											

CHANGE LETTER	DRAWN BY	CHECK BY	DATE	CHANGE
B	[illegible]	[illegible]	4-17-49	REDESIGNED

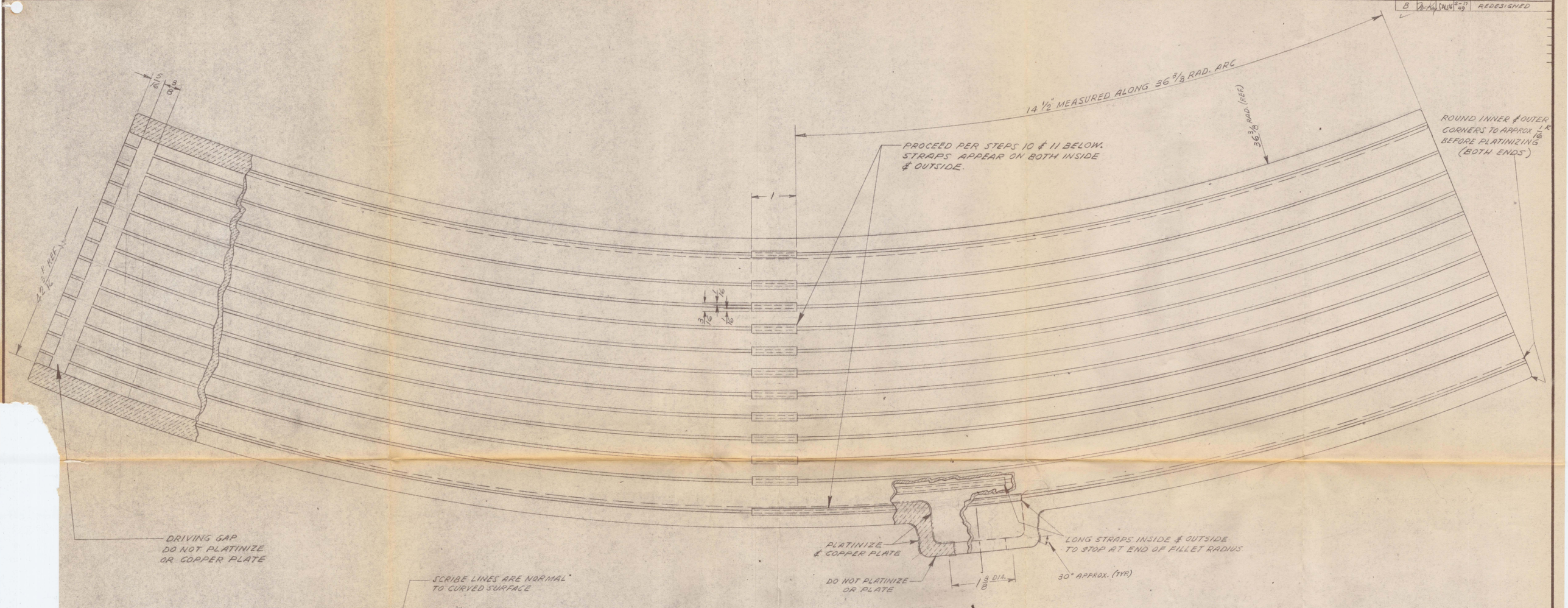

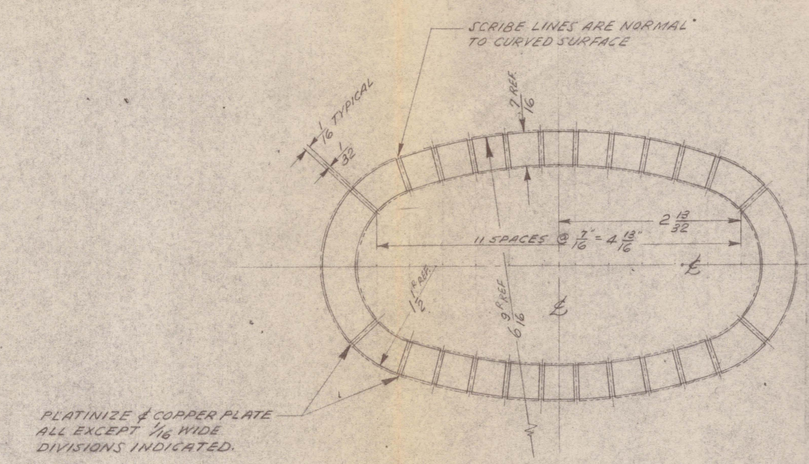

END VIEW OF SEGMENT

TYPICAL OF BOTH ENDS

R. F. SEGMENT PREPARATION PROCEDURE

1) Grind off all sand and projections on inside surface. Cover ends using black rubber gaskets backed up by copper plates. Fill inside with hydrofloric acid, taking care that no air is trapped. Allow hydrofloric acid to remain in segment for 8 hours.

2) Grind ends and outside per 4C8593B. Grind boss per 4C5782C. In addition, wall thickness must be uniform within 1/16 inch. If necessary, grind outside to obtain this uniformity.

3) Wash in alcohol and fire at 1300° F. Take 4 hours to reach this temperature and 12 hours to cool from it.

4) When quartz has cooled to room temperature, paint all except driving gap and areas of boss indicated with thin, uniform coat of Hanovia 05 Liquid Bright Platinum. Allow to air dry for 1 hour. Fire for 15 minutes at 1300° F in an oven with forced air circulation. Take 4 hours to reach 1300° F and 12 hours to cool.

5) Apply 2nd coat as above.

6) Using a meter and probes, make a comprehensive continuity check of the platinum coating. Coat any open spots with platinum solution and fire.

7) Using striping machine 4C5644, roll on 1/16" wide stripes of red glyptal per detail at left.

8) Copper plate in copper sulphate solution. Flash at 15 amps plating current. Use a portable probe to cover areas not adequately flashed with fixed electrodes. After flashing, decrease current to 8 amperes and plate until copper coating is .006 ± .0005 thick. Coating must be uniform - use care to prevent heavy deposit on edge.

9) Wash off glyptal in methyl ethyl ketone. Using a motor driven 1/32 thick by 3/4 dia. "Handee" carborundum disk, clean up all division lines. Use flexible shaft and 90° head when cleaning inside lines. Remove as little of the silica body as possible. After grinding, burn out any residual plating between straps. Use a 5 volt 200 amp filament transformer with Variac on 110 volt input side. Next use a 110 volt Variac in series with a 25 watt light bulb. Continue until resistance between copper straps is greater than 100,000 ohms.

10) Using red glyptal, coat all except the 3/16 x 1 connecting straps which appear approximately at the center of the segment. Leave 1/16" of copper showing on each side of the unplated groove. Bridge over the unplated portion with 4817 DuPont air drying silver, allowing silver to overlap copper 1/32 on each side. 1/32 of copper to be left exposed between silver and glyptal. (USE 3 COATS OF GLYPTAL)

11) Copper plate .002 thick over connecting straps only.

12) Remove glyptal with methyl ethyl ketone.

REFERENCE DRAWINGS

1) SEGMENT MOLDING DETAIL: 4C3074C
2) R.F SEGMENT MOLDING DETAIL (1 SPECIAL OUTSIDE BOSS): 4C8602B
3) " " DRIVING BOSS GRINDING DETAIL: 4C5782C
4) "STOP-OFF" STRIPING HEAD CARRIER FRAME: 4C5844
5) "STOP-OFF" STRIPING HEAD ASS'Y.: 4C5682
6) OSCILLATOR & TRANSMISSION LINE ASS'Y.: 5C4965A
7) SEGMENT GROUNDING DETAIL: 4C9134B
8) SEGMENT GRINDING DETAIL: 4C8593B
9) INJECTOR & PUMP SEGMENT (2 OUTSIDE TUBUL.): 4C3082B
10) PROBE SEGMENT (1 OUTSIDE TUBUL.): 4C3092B
11) TARGET SEGMENT (1 INSIDE TUBUL.): 4C3112B
12) BLANK SEGMENT (NO TUBUL.): 5C7521
13) SEGMENT TUBULATION (ONLY): 5C7491

SYNCHROTRON - SERIES B VACUUM CHAMBER
R. F. SYSTEM
R F SEGMENT PLATINIZING & COPPER PLATING

FIRST USED ON JOB NO. 144-4

RADIATION LABORATORY
UNIVERSITY OF CALIFORNIA–BERKELEY

DRAWN BY [illegible] CHECK BY [illegible] DATE 2-16-49
APPROVED BY
SCALE FULL SIZE
DRG. NO. 4C5984B

TOLERANCES WHERE NOT OTHERWISE GIVEN

ISSUED TO	DATE ISSUED	DELIVER TO	JOB NO.	DATE REQ'D	MAKE

1951 K. & E. CO., N. Y.

eRecordsUsa

eRecordsUsa

eRecordsUsa

eRecordsUsa

eRecordsUsa

eRecordsUsa